To the Graduate Council:

I am submitting herewith a thesis written by Patricia R. Taft entitled "Examinations Of A Helmholtz Resonator For Use In Enhancing Hybrid Fuel Grain Regression." I have examined the final copy of this thesis for form and content and recommend that it be accepted in partial fulfillment of the requirements for the degree of masters, with a major in Aerospace Engineering.

Frank G. Collins, Major Professor

We have read this thesis and recommend its acceptance:

Accepted for the Council:

Associate Vice Chancellor
and Dean of The Graduate School

STATEMENT OF PERMISSION TO USE

In presenting this thesis in partial fulfillment of the requirements for a Master's degree at The University of Tennessee, Knoxville, I agree that the Library shall make it available to borrowers under rules of the Library. Brief quotations from this thesis are allowable without special permission, provided that accurate acknowledgment of the source is made.

Permission for extensive quotation from or reproduction of this thesis may be granted by my major professor, or in his absence, by the Head of Interlibrary Services when, in the opinion of either, the proposed use of the material is for scholarly purposes. Any copying or use of the material in this thesis for financial gain shall not be allowed without my written permission.

Signature Patricia R Taft

Date 4-28-94

EXAMINATION OF A HELMHOLTZ RESONATOR FOR USE IN ENHANCING HYBRID FUEL GRAIN REGRESSION

A Thesis

Presented for the

Master of Science

Degree

The University of Tennessee, Knoxville

Patricia R. Taft

May 1994

DEDICATION

This thesis is dedicated to my husband, Kris S. Taft,
who has provided me with motivation when I was sure there was none.

ACKNOWLEDGEMENTS

Dr. Frank Collins, my major professor, and advisor, helped me in achieving my goals through his unlimited amount of joy and enthusiasm he imparts in his teaching and research.

Dr. Basil Antar fostered my devotion to fluid dynamics through the immense amount of support he gave me over the past two years. He is an excellent teacher and has given me very good advise and an abundant amount of his time.

In gathering my data I had the help of Ricky Meeker, Harold Sartain, Jim Goodman, Bill Millard, Gary Payne, and Wes McMinn. I value their teaching, assistance and patience as I created my resonator and motor apparatus. I am especially grateful for the amount of effort Ricky, Jim and Gary for their significant assistance under difficult conditions. Without their dedication there would be no data for this thesis.

This research was partially supported by the Tennessee Space Grant Consortium, NGT 40021. It was awarded to Vanderbilt University who subcontracted it out to The University of Tennessee Space Institute. Equipment support was also supplied by the National Aeronautics and Space Administration (NASA).

ABSTRACT

The use of a Helmholtz resonator, placed in the oxidizer line upstream of the injector, to supply disturbances in the precombustion chamber of a hybrid rocket motor was examined. The intent was to disturb the combustion turbulent mixing with a resonant frequency of the Helmholtz resonator, hence to increase the hybrid fuel regression rate.

For these studies a hybrid rocket motor, test stand, oxidizer feed line, and Helmholtz resonator were constructed. Only cold flow tests were performed, using high pressure air as the test media.

The characteristics of the Helmholtz resonator were determined by placing a condenser microphone within the resonator and on the oxidizer feed line opposite to the resonator. Frequency spectra were measured for various resonator geometries as a function of the oxidizer line mean velocity.

The measured sound power level due to the Helmholtz resonator was in the same range as the measured noise inherent in the entire system. Lack of a distinct resonant frequency, stronger than the system noise, indicates that the Helmholtz resonator configuration used herein will not produce a resonant frequency strong enough to increase the fuel burn rate of a hybrid rocket engine. Thus, other passive means must be found to disturb the oxidizer flow strongly enough to have an influence on the fuel regression rate. One such design namely a protuberance into the oxidizer line displayed a definite peak in the frequency in the precombustion chamber. Such designs, which may be more successful, need to be pursued.

TABLE OF CONTENTS

LIST OF TABLES

LIST OF FIGURES

LIST OF SYMBOLS

A - cross-sectional area of the oxidizer line

A_t - nozzle throat cross-sectional area

B & K - Bruel & Kjœr

D_p, D_{pipe}- oxidizer line diameter

H - cavity length

P* - pressure at the throat when flow is choked

P_{atm} - atmospheric pressure

P_t - total pressure

P' - pressure due to perturbation of sound waves in the flow

P'_{rms} - resonator cavity pressure measured by Spectrum Analyzer

P_s - static pressure

P_1 - static pressure measured upstream of resonator

P_2 - static pressure measure at post combustion chamber

ΔP - P_t - P_s

Re - Reynolds number

Ru - universal gas constant

S_o - resonator aperture cross-sectional area

S - cavity cross-sectional area

Str - Strouhal number

SPL - sound pressure level

T - period

T_{atm} - atmospheric temperature

U - free stream velocity

V_o - resonator aperture volume

V - resonator cavity volume, not including the neck

$V' = V + V_o$

c - speed of sound

d_o - aperture diameter

d - cavity diameter

f_o - resonant frequency

$(f_o)_t$ - Panton's theoretical resonant frequency

f - frequency

h - height of protrusion in a flow

l_1, l_2 - two parts to the total end correction

l_v - form factor

l' - effective length or ength correction of aperture thickness

n - wave number

q - dynamic pressure of freestream

t - resonator aperture thickness

$t' = t + l_1$

Δ_i - length correction inside resonator cavity

Δ_o - length correction outside resonator cavity

M_{air} - molecular weight of air

α – end correction length

λ - wavelength

μ - viscosity

θ – angle between the sound source and the point where its observed

ρ- density

ω - angular frequency

LIST OF EQUIPMENT

1. QC-10 Microphone Calibrator, 114 dB - 1000 Hz, SN QE2080047, Quest Electronics, Oconomowoc, Wisconsin.

2. Fluke 51 K/J Thermometer, SN 5550681, John Fluke Manufacturing Company, Inc., Everett, Washington.

3. Pressure Gauge, Scale: 0 - 300 psi, WIKA.

4. 3582A Spectrum Analyzer, SN 1809A02263, Hewlett Packard, California.

5. Type 2112 Audio Frequency Spectrometer, SN 227998, Bruel & Kjœr, Copenhagen, Denmark.

6. Cartridge Type 4136 Condenser Microphone, 1/4" diameter, SN 533391, Bruel & Kjœr, Copenhagen, Denmark.

7. Dynamic Pressure Transducer, Model 8510C-15, SN G08G, Endevco, San Juan Canistrano, CA.

8. 7035B, X-Y Recorder, SN 1206A07216, Hewlett Packard, California.

9. Model No. FA 145, Pressure Gauge, Scale: 0 - 4.3 psi, SN 19162, Wallace & Tiernan, Belleville, NJ.

10. Model No. FA 145, Pressure Gauge, Scale: 0 - 120 inches H_2O, SN WP 59626, Wallace & Tiernan, Belleville, NJ.

11. Model No. FA 145, Pressure Gauge, Scale: 0 - 5000 psf, SN 10054 B, Wallace & Tiernan, Belleville, NJ.

CHAPTER I

INTRODUCTION

Recently there has been a renewed interest in the hybrid rocket motor. The hybrid motor combines a liquid oxidizer and a solid fuel into a single system. The advantages of using the hybrid rocket motor, instead of the liquid or solid rocket motors, outweigh its disadvantages, although the latter should not be ignored. Some of the advantages of the hybrid include: it is much safer to build, store or operate because it cannot explode; it is environmentally safe; the fuel and oxidizer are stored separately, the flow of the oxidizer is controllable, and the fuel is inert by itself, hence the hybrid motor can be shut down any time during operation simply by cutting off the flow of the oxidizer; and the total costs are significantly lower compared to traditional rocket motors because of its inherent safety. Also, during operation, due to the controllable oxidizer flow, it can be throttled smoothly through a wide range of thrusts thus making it comparable to a jet engine in terms of thrust response. The hybrid motor is also more reliable than either the liquid or solid rocket motor. In comparison to the liquid motor, hybrids contain half the pumps and plumbing, since just one liquid is used. Compared to solid rocket motors, hybrids have a stronger and inert fuel grain. Also there is no overpressure due to defects that sometimes occur in solid propellant grains. Finally, the hybrid has a higher specific impulse than solid rocket motors, and higher-density impulse than liquid motors.

On the other hand, the hybrid rocket motor also has disadvantages compared to traditional motors. The fuel regression rate and mass fraction are lower compared to solid rocket motors, and the combustion can become unstable. Some other disadvantages include a moderately uncontrollable mixture ratio that causes a varying specific impulse during steady-state operation and throttling, and a steady-state combustion efficiency which can fall into the 93-97% range, which is slightly lower than for both liquid and solid rockets. The lower performance of hybrid motors is due to the lower fuel regression rate; the hybrid regression rate is about two-thirds of that found for solid motors (Sutton, 1992).

Presently, to make up for the lower fuel regression rate, the hybrid has a much larger burn surface area incorporated into the fuel grain design. This is accomplished using a multi-port fuel grain. To improve thrust this type of grain allows for an increase in the mixing of the fuel and oxidizer by increasing the possible surface area of burning, but it results in a poor mass fraction.

The low regression rate problem is not solved by increasing the surface area of burning; its significance is just reduced. The regression rate needs to be increased in order for the hybrid to outperform the solid motor. One solution to this problem would be to increase the mixing rate of the oxidizer and fuel. Like a candle, the solid fuel in the hybrid must vaporize before it can begin to burn, but the actual vaporization is very limited.

The purpose of this study is to determine if a Helmholtz resonator placed upstream of the precombustion chamber could increase the flame front turbulent mixing rate as another approach to the problem. The benefit of the Helmholtz resonator is that its resonance frequency can be predetermined by the resonator geometry alone according to previous experiments and theory. If this is possible, then it should also be possible to preset the resonator to a resonance frequency that would produce the highest amount of turbulent

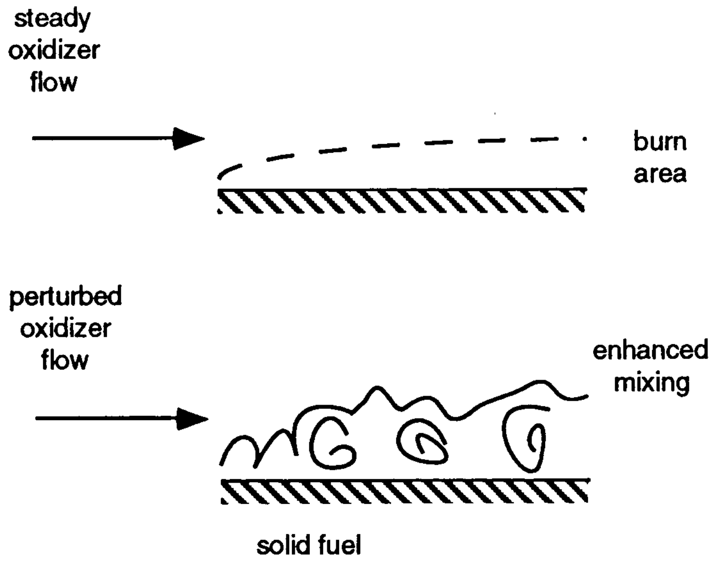

mixing in the hybrid fuel grain flame front thus increasing the regression rate of the fuel.

The main idea was to disturb the oxidizer flow. The first idea was to disturb a portion of the oxidizer input to the precombustion chamber, by rotating a modified ball valve. A high-pressure ball valve was purchased to see if it could be modified for use on the oxidizer line. It was desired to disturb the flow at a frequency of about 500 Hz. The handle was removed and Teflon seals were placed around the shaft. The valve was opened and closed at this high speed using a motor attached to the shaft. The test was unsuccessful since the valve became hot and destroyed the seal. Since a hot valve could not be used on an oxidizer line it was decided that a more passive way of disturbing the flow was needed, hence the Helmholtz resonator. Since there are no moving parts in the resonator there would be little chance of mechanical failure, and no chance of preheating the oxidizer.

CHAPTER II

LITERATURE REVIEW

A child swinging on a swing needs some help in order to swing higher. You push with the swing's motion, allowing it to travel higher than it could alone. You are addng to the motion of the swing, increasing its maximum height, or amplitude. Then the child wants to get off. You push against the swing's motion, decreasing its amplitude. Likewise, a Helmholtz resonator can also be used to either enhance or decrease a disturbance at the resonant frequency of the system it is incorporated into. The type of Helmholtz resonator considered in this literature review was designed to enhance a disturbance at the frequency of the resonator. This disturbance was then to be introduced into the precombustion chamber of a hybrid rocket motor.

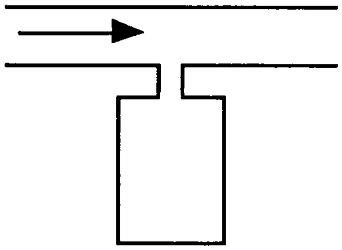

A Helmholtz Resonator As A Branch On A Pipe

The resonant frequency of the Helmholtz resonator is dependent on its geometry and the speed of sound. An extensive amount of theoretical and experimental research on the Helmholtz resonator has been accomplished over the past century, initially developed by Helmholtz in 1860 (Rayleigh, 1945).

This literature review was limited to the type of Helmholtz resonator that is connected perpendicularly to a pipe and is excited by the turbulent flow in the pipe. Several authors have derived variations of an equation for this type of resonator. (Rayleigh, 1945, Kinsler & Frey, 1962, Alster, 1972, Panton, 1975 & 1990, and Dowling & Ffowcs Williams, 1983.) A discussion of a few of their theories and experimental data follows.

In the nineteenth century, the theoretical equation for the resonant frequency that was generally accepted is:

$$f_o = \frac{c}{2\pi}\sqrt{\frac{S_o}{t\,V}} \tag{2.1}$$

or, since $\omega_o = 2\,\pi\,f_o$,

$$\omega_o = c\sqrt{\frac{S_o}{t\,V}}$$

where

f_o - resonant frequency

c - speed of sound

S_o - resonator neck cross sectional area

t - resonator neck length

V - resonator cavity volume, not including the neck

ω_o - angular frequency

This equation is only valid for long neck resonators. It fails for thin apertures, because the resonant frequency can never reach infinity. Rayleigh derived an end correction length defined as $\alpha = 0.8$ d, where d is defined as the resonator cavity diameter. The air moves through the neck as a single mass, remaining so for a short distance after exiting. The end correction length is this distance. This end correction length, a modified neck length, prevents the resonant frequency from going to infinity, as the neck length becomes very short. Based on theory, Helmholtz derived the end correction length for an open end as:

$$\alpha = 0.125\,\pi\,d_o$$

where d_o is defined as the aperture diameter (Rayleigh, 1945). Although Rayleigh hints that Helmholtz's derivation of the end correction length, α, is incorrect, he does admit that it fits experimental data. Thus, Rayleigh incorporated it into his own resonant equation, which is:

$$f_o = \frac{c}{2\pi}\sqrt{\frac{S_o}{V\left\{t + \frac{1}{2}\sqrt{\pi S_o}\right\}}} \qquad (2.2)$$

or simply

$$f_o = \frac{c}{2\pi}\frac{d_o}{d}\sqrt{\frac{S_o}{H\left\{t + \frac{\pi}{4}d_o\right\}}} \qquad (2.3)$$

where H is defined as the resonator cavity length, not including the aperture thickness. This equation works very well for short, as well as long, neck resonators. As t gets larger the correction factor becomes negligible. This will give us the original resonator equation, valid for only long neck resonators (Rayleigh, 1945).

In the text, Kinsler & Frey, 1962, a different approach is taken, hence, a different end correction length is derived. The equation they introduce is:

$$f_o = \frac{c}{2\pi}\sqrt{\frac{S_o}{l' V}} \qquad (2.4)$$

(Kinsler & Frey, 1962). This equation assumes that the flow through the aperture is incompressible, and that the geometric dimensions are much smaller than the wavelength, λ, where

$$\lambda = \frac{c}{f_o}.$$

Kinsler & Frey assumed that the Helmholtz resonator, an acoustic system, is analogous to a mass-spring system. The pressure in the resonator cavity, either under compression or expansion, represents the massless spring, while the air mass moving through the aperture represents the mass of the system. The pressure, like the spring, moves the mass in and out of the aperture. The authors also include a resistance element, that occurs because the mass, moving out of the cavity, experiences a decreased velocity due to friction between it and the gas in the outer surroundings. Hence, kinetic energy of this acoustic system must decrease. This implies that the system sustains an energy loss due to dissipation, or viscous effects. Because of zero velocity along the surface of the aperture wall, and its small diameter, there is also a resistance due to the air mass moving past the inner wall of the aperture that may not always be neglected, depending on the diameter. It is noted that if the aperture diameter is less than one centimeter then the friction due to the air interacting with the wall of the aperture will be greater than that due to the outer air resistance (Kinsler & Frey, 1962, p. 187). Assuming that the acoustic resistance is greater, the authors also state that the resonator is comparable to a piston. If this is true then the effective length can be written as:

$$l' = t + 2\Delta t = t + \frac{8\, d_o}{3\pi} \qquad (2.5)$$

where t is defined as the thickness, or length, of the aperture of the resonator (Kinsler & Frey, 1962). Therefore, equation (2.4) can be rewritten as:

$$f_o = \frac{c}{2\pi}\frac{d_o}{d}\sqrt{\frac{1}{H\left\{t + \frac{8}{3\,\pi}\,d_o\right\}}} \qquad (2.6)$$

The mass-spring system to acoustic system analogy was not new. Rayleigh discusses it in his book, previously mentioned. He originally published his book containing his Helmholtz resonator equation derivation back in 1896. In his 1972 paper, Alster starts with the same analogy, but his spring, the pressure compressions and expansions that occur within the cavity, is no longer assumed massless. He offers a fully detailed derivation, beginning with the equations of motion. But Kinsler & Frey's adjustment is an end correction length. Alster's equation has three assumptions behind it. First, his equation is:

$$f_o = \frac{c}{2\pi}\sqrt{\frac{S_o}{1.21\,(V + V_o)\left\{\frac{V}{V+V'}\frac{H}{H+t'}\left[l_V + (t')\left(1 + \frac{1}{2}\left[\frac{V'}{V} + \frac{t'}{H}\right] + \frac{1}{3}\frac{V'}{V}\frac{t'}{H}\right)\right] + l_2\right\}}} \qquad (2.7)$$

where

$$V' = V_o + V_1$$

$$t' = t + l_1$$

$$V_1 = S_o \, l_1 \text{ or,}$$

$$V_1 = 0.3 \, \pi \, d_o^2$$

and

$$l_v = \frac{S_o}{V \, H} \int_0^H \frac{x \, V(x)}{S(x)} \, dx \qquad (2.8)$$

where x is any point along the cavity length. The value V_1 is defined as the volume of the hypothetical elongation of the neck due to the motion of the gas particles outside the resonator. The value, l_v, is defined as the form factor because it is dependent on the cavity shape. The terms, l_1 and l_2, are two parts of the total end-correction length. They depend on the motion of gas particles that occur outside the resonator. Alster expanded on this end-correction length. He derived it and made the assumption, using the spring-mass system analogy, that the volume of air in the neck is the mass of this acoustic system, and the volume, that experiences the changing pressure in the cavity, acts as the spring. He does not make the assumption that the spring is massless, however. He claims any spring that can move a mass must have mass itself. Starting the derivation without the massless spring assumption surely complicates the mathematics but it is no longer necessary to empirically find the end-correction length. Likewise, he did not make the assumption that the cavity shape has no effect on the resonance frequency. He experimentally proved that there is a dependency of frequency on the volume by performing a very simple experiment using a bottle. He poured a small amount of fluid into the bottle, then blew across the opening. Then he tilted the bottle a little, and blew over it again. The resonator still had the same volume but no longer the same shape. He didn't hear a change in the pitch until he had the bottle nearly horizontal. Alster also took equation (2.7) one step further, in his paper, by deriving what the form factor l_v would be for several particular shapes. For the cylinder shape, he found that

$$l_v = \frac{H S_o}{3 S} \qquad (2.9)$$

where S is defined as the resonator cross-sectional area. He also found, by experiment, that in most cases, it is safe to assume that

$$l_1 = l_2 = 0.12\, d_o,$$

though it is best to keep in mind that these lengths can slightly vary from each other due to changes in the pipe arrangement that the resonator is attached to. Alster assumed that the resonator is symmetrical about the neck axis, that any dimension D′ of the resonator should be within the limits $D' < 0.25 < \lambda$, and that the resonator length remains larger than the resonator neck diameter. Beyond these three limits, the resonance frequency equation may lose some of its accuracy (Alster, 1972).

Another research on the Helmholtz resonator is given by Panton, 1975 & 1990. He presented two equations in his 1975 paper, that predict both the fundamental resonance frequency, and its higher modes. This equation also does not break down if the resonator length, H, reaches, or goes beyond, one-sixteenth of the wavelength of the system, as he found to occur for the resonator equations like equation (2.6). Panton uses an equation that gives all resonant wavenumbers:

$$\frac{l' S}{H S_o} n H = \cot(n H) \tag{2.10}$$

where

$$\cot(n H) = \frac{1}{n H} - \frac{1}{3} n H - \frac{1}{45} (n H)^2 - \cdots \tag{2.11}$$

and

$$n = \frac{2 \pi}{\lambda} = \frac{2 \pi f_o}{c} \tag{2.12}$$

and, by neglecting the higher order terms, this equation simplifies to:

$$\cot(n H) = \frac{1}{n H} - \frac{1}{3} n H \tag{2.13}$$

(Refer to Panton's paper, 1975, to see plots of this equation.) Panton uses this in conjunction with the Helmholtz resonator equation:

$$f_o = \frac{c}{2\pi} \sqrt{\frac{S_o}{l' V + \frac{H^2 S_o}{3}}} \tag{2.14}$$

where l' is the effective length. The effective length is the length of the neck and the end-correction length combined. He derived the effective length based on Rayleigh's outside correction and Ingards inside correction (Rayleigh, 1945 and Ingard, 1954). Panton's mathematical definition of the effective length is:

$$l' = t + \frac{4 d_o}{3 \pi} \left[2 - 1.24 \frac{d_o}{d} \right] \tag{2.15}$$

where the second term on the right-hand side is the end-correction length. Refer to Ingard's paper for aperture diameter's larger than $d_o < 0.4d$. Panton discovered that the cavity pressure, measured with a microphone inside the cavity, would reach a maximum when the nondimensional freestream velocity was:

$$\frac{U}{d_o f_o} \approx 3.5 \text{ to } 4.0 \qquad (2.16)$$

where U is the freestream velocity. Panton tested his in a wind tunnel, with turbulent flow, at velocities between 30 and 160 mph. He found that, as the wind tunnel velocity was increased, the turbulent noise of the system would dominate the sound power output of the resonator. He also found in his experiments that the sound pressure level at the resonant frequency increases slowly with increasing wind tunnel velocity but the increase is of the order of 10^{-2}.

Dowling & Ffowcs Williams, 1983, in addition to the Helmholtz resonator equation, present an equation that can be used to predict the pressure variation in the oxidizer pipe flow due to the resonator compressions and expansions. (Refer to Figure 2.1.) The equation is for flow over a vibrating piston, but the air moving in and out of the aperture is analogous to the piston, illustrated in Figure 2.1 with a double arrow. The equation is

$$P'(\mathbf{x}, t) = \frac{A\,B}{|\mathbf{x}|\left(1 + M\cos\theta\right)^3} \exp\left[\frac{\iota\,\omega\left(t - \frac{|\mathbf{x}|}{c}\right)}{1 + M\cos\theta}\right] \qquad (2.17)$$

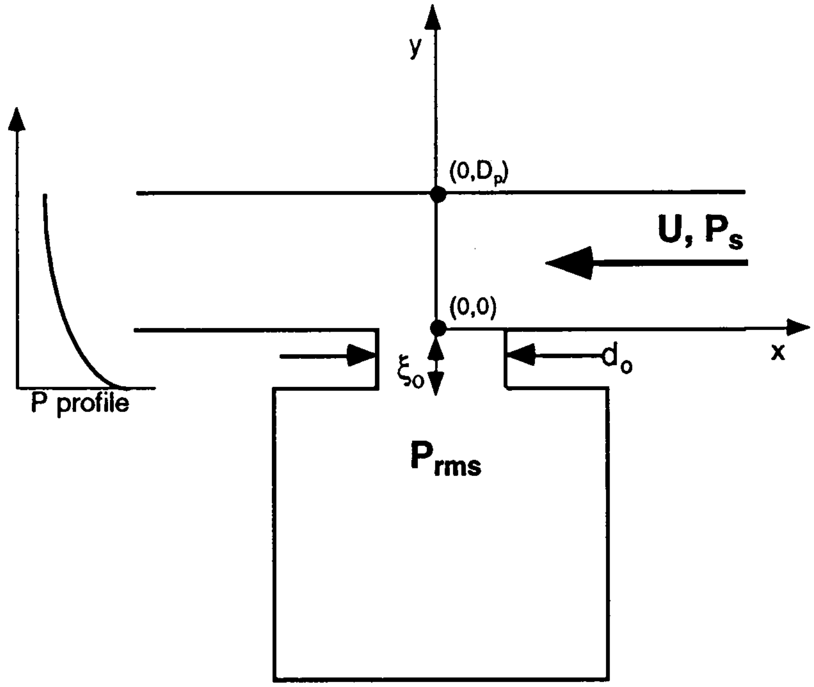

Figure 2.1 Pressure Variation In Oxidizer Line And Helmholtz Resonator

where **x** represents two dimensional space and

$$|\mathbf{x}| = \sqrt{(x^2 + y^2)}$$

therefore, for a Helmholtz resonator

$$|\mathbf{x}| = D_p \tag{2.18}$$

where D_p is the oxidizer pipe diameter.

Also,

$$A = \frac{-(2\pi - 4)}{\pi^2}$$

or simply $A = -0.231$, and

$$B = \frac{\rho_o \, \xi_o \, \omega^2 \, d_o^{\,2}}{4}$$

then, since $\omega = 2\pi f$,

$$B = \pi^2 \rho_o \xi_o f^2 d_o^2$$

where, from the mass-spring model, $\xi = C_o \sin \omega t$, ξ_o is the maximum amplitude. Also

M - mach number of the freestream

ω - angular frequency

θ - angle between the sound source and the point where its observed

ρ_o - density of the freestream flow.

From equation (2.17) P'_{rms} can be calculated knowing

$$P'^2_{rms} = \overline{P'^2} \tag{2.19}$$

and

$$\left(\overline{P'^2}\right) = \frac{1}{T}\int_0^T P'^2 \, dt. \tag{2.20}$$

The Mach number may be neglected since the velocity in the pipe flow is very small compared to the speed of sound. This is a valid assumption since the velocity is measured at a point upstream of a choked exit nozzle. Hence, the equation (2.17) can be rewritten as

$$P'(\mathbf{x}, t) = \frac{-0.23\,B}{|\mathbf{x}|} \exp\left[t - \frac{|\mathbf{x}|}{c}\right]$$

From this P'_{rms} can be determined using equation (2.20) eliminating time t.

$$\overline{\left(P'^2\right)} = \frac{1}{T}\int_0^T \left\{\frac{-0.23\ B}{|\mathbf{x}|}\exp\left[\iota\,\omega\left(t - \frac{|\mathbf{x}|}{c}\right)\right]\right\}^2 dt.$$

The modulus of $(e^{\iota x})^2$ is

$$(e^{\iota x})^2 = \cos^2 x + \sin^2 x = 1,$$

therefore

$$\overline{\left(P'^2\right)} = \frac{1}{T}\left[\frac{-0.23\ B}{|\mathbf{x}|}\right]^2 \int_0^T dt.$$

From equation (2.19)

$$P'^2_{rms} = \overline{\left(P'^2\right)} = \left[\frac{-0.23\ B}{|\mathbf{x}|}\right]^2$$

hence

$$P'_{rms} = \frac{0.23\ B}{|\mathbf{x}|}.$$

This equation states that as $\mathbf{x} \to \infty$ $P' \to 0$. It should be noted, however, that this equation is for a uniform flow over the piston while the present experiment included a boundary layer. It can be expected that this boundary layer would further attenuate the far field pressure fluctuations. Also, this equation is for a piston vibrating in free space where $\mathbf{x} \to \infty$ while in the case of the Helmholtz resonator the mass of air in the aperture is confined to the space where $\mathbf{x}_{max} = (0, D_p)$.

For the coordinate system of the Helmholtz resonator defined in Figure

2.1 this becomes

$$P'_{rms} = \frac{0.23\,B}{D_p} \tag{2.21}$$

which should be compared with the pressure measured by the Spectrum Analyzer when the microphone is located at $(0, D_p)$ as in Figure 2.1.

CHAPTER III

EXPERIMENTAL PROCEDURES

A. INITIAL APPARATUS FABRICATION AND INSTALLATION

For this experiment a Helmholtz resonator was placed 9.66 inches upstream of the hybrid rocket motor. (Refer to Figure 3.1.) All tests to be reported were performed without combustion. The motor casing was constructed of a three-inch diameter, schedule 80, stainless steel pipe. (Refer to Figure 3.2.) One each, three-inch, schedule 80, stainless steel, slip-on flange was welded to each end of the motor casing. For the solid fuel, a bar of cast plexiglass, cut to an 18-inch length, was machined to fit inside the motor, and a one-inch hole was drilled lengthwise through its centerline. It was placed inside the motor casing, leaving a three-inch length space forward of it, and a seven-inch length space aft. A line of RTV was placed around the outer diameter of the plexiglass at its forward cross-sectional plane preventing the air from flowing through. A 2.5-inch, schedule 160, PVC pipe, cut to a seven-inch length, was installed in the seven-inch length aft section. A one-inch hole was drilled through the center of a blank flange onto which the motor nozzle was attached. An exit nozzle, with a 0.26-inch throat diameter, and a 0.6-inch exit plane diameter, was installed in the hole. The nozzle, made out of steel and graphite, fit into this hole. The flange, with the nozzle, was bolted onto the aft end of the hybrid motor.

An injector was constructed out of a stainless steel one-quarter cup measuring cup with its handle machined off. It was one-inch in length, streamwise. It was placed in the forward end of the motor, with its open end in

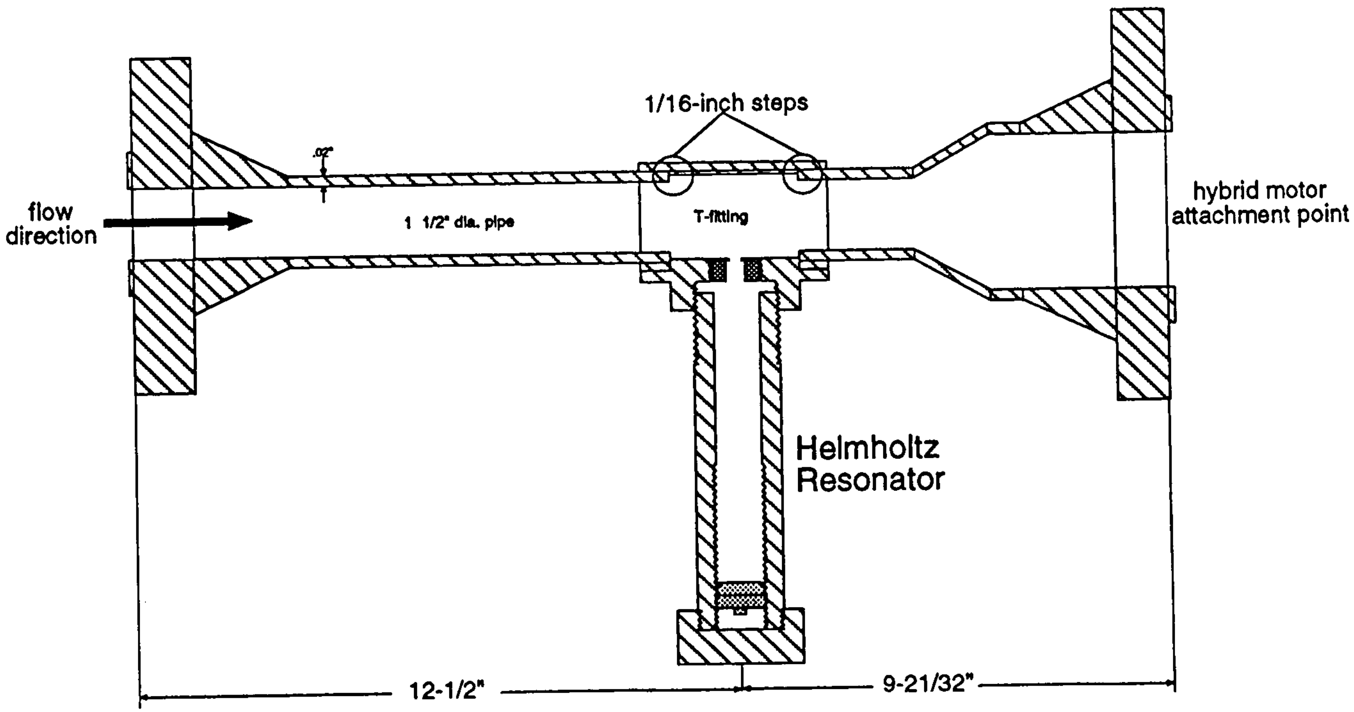

Figure 3.1 Placement Of Helmholtz Resonator

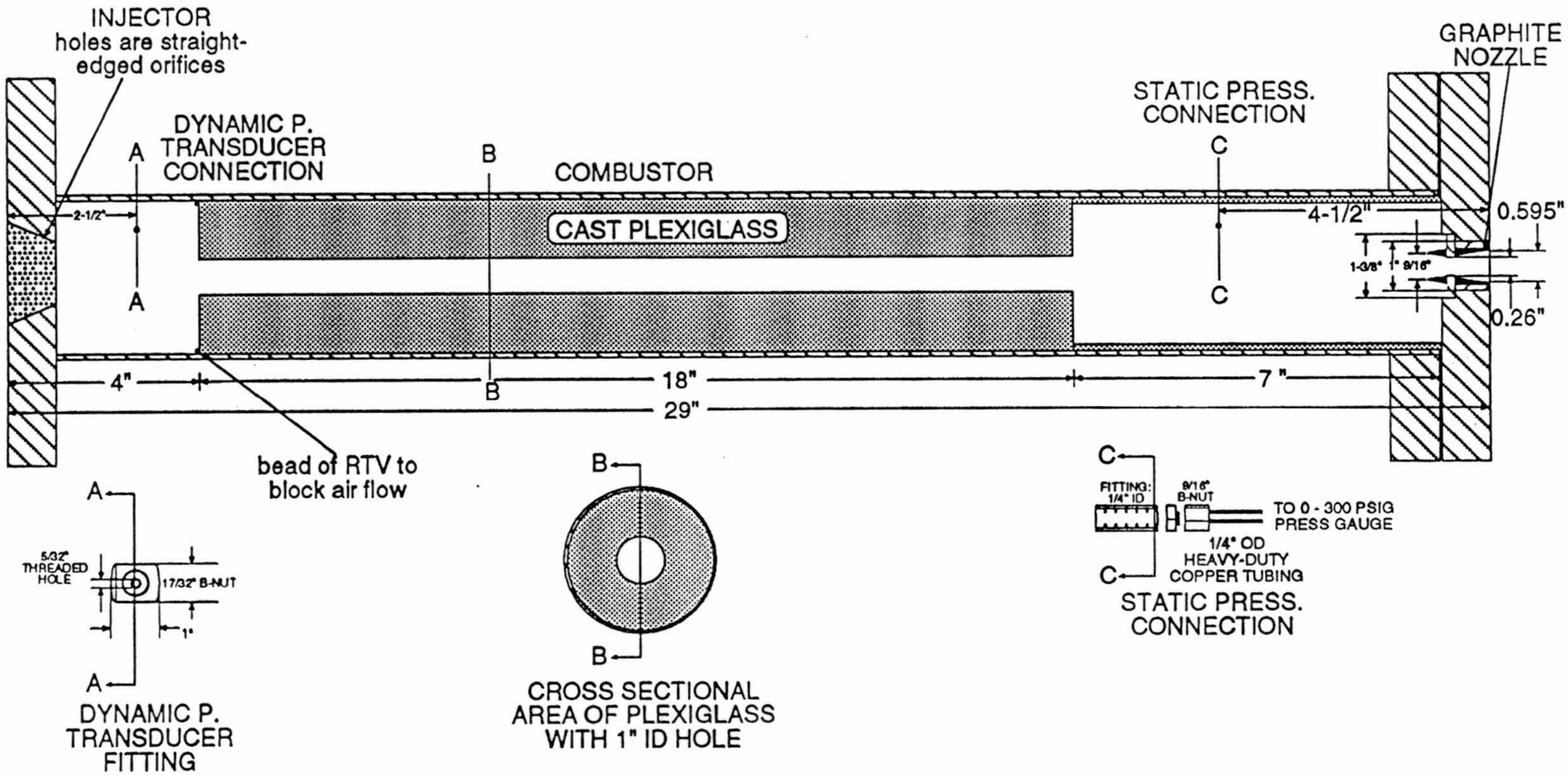

Figure 3.2 Hybrid Rocket Motor

the cross-sectional plane of the forward end of the forward slip-on flange. Its length was the same as the thickness of the flange it was placed in. The injector had thirteen eighth-inch diameter holes drilled through it: four holes, evenly spaced around the circumference of its circular side wall and eight evenly spaced around a ninth center hole through its bottom. Note that the bottom of the cup faced downstream. The bottom was 1.44 inches in diameter, and the open top section was 2.31 inches in diameter. A spacer was constructed to hold the injector in place. The spacer had a three-inch outer diameter, and a 2.31-inch inner diameter. The injector fit tightly into this spacer. The outer diameter of the spacer was held in place in the pipe's front cross-sectional plane with RTV.

The Helmholtz resonator was constructed out of stainless steel, schedule 160, one-inch diameter pipe. (Refer to Figure 3.3.) Its full length was 9.75 inches with a maximum cavity length of 7.44 inches, and an inside diameter of 1.06 inches. A set of quarter-inch long solid, stainless steel spacers were machined to fit into the resonator cavity in order to change its length. Female threads were cut into the aft end of the cavity. A plug, with male threads, was constructed to thread into the cavity aft end. This plug was made to hold the quarter-inch spacers in place. One spacer had a groove machined into its outer diameter. A 0.70-inch thick, one-inch outer diameter O-ring was installed in the groove. This spacer that would be the bottom, or floor, of the cavity, was fabricated to prevent air leakage. Eventually, because the spacers kept getting stuck within the cavity, due to their thinness, much thicker spacers were machined, i.e., a seven-inch piece, a six-inch piece, etc., which solved the problem. The grooved spacer was kept as the cavity floor. A female threaded endcap was screwed onto the threaded aft end of the

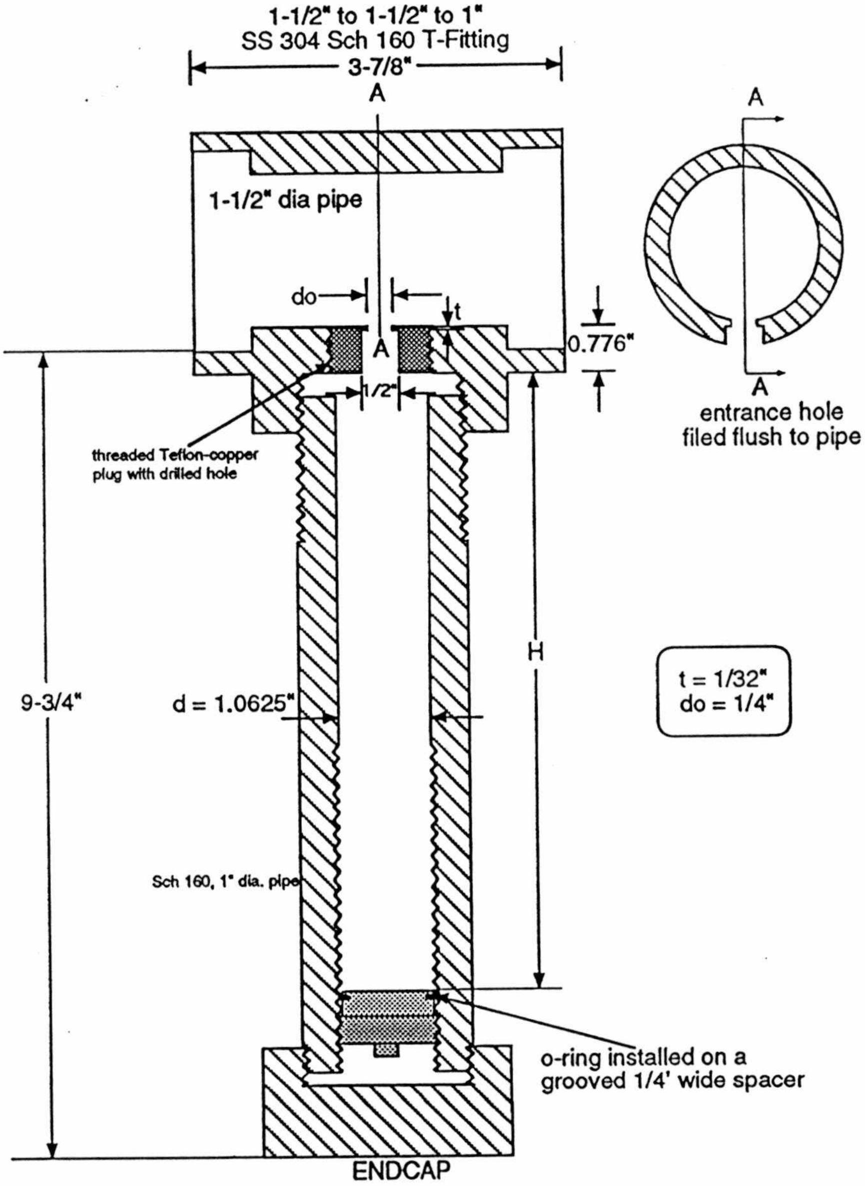

Figure 3.3 Helmholtz Resonator Attached To Stainless Steel T-Fitting

resonator cavity body.

The Helmholtz resonator cavity had male threads cut into its forward pend. It was then screwed into the branch of a T-fitting. (Refer to Figure 3.1.) The T-fitting was a 1.5-inch by 1.5-inch diameter, with a one-inch branch. Two sets of female threads were cut into the branch of the T-fitting. This T-fitting had a branch that was 1.13 inches long, from the edge of the main pipe line to the edge of its cross-sectional opening. Within this was a step, with the smaller diameter being the one that meets the pipe line. Female threads were machined into these, and a one-inch diameter plug, constructed out of Teflon-copper mix bar stock, was machined and threaded to screw into this threaded section. This 0.78-inch thick plug had a quarter-inch diameter hole drilled through its center line. This hole was the aperture of the resonator. In order to make the thickness of the aperture 0.01 inches, a second, half-inch flat bottom hole was drilled through the center, stopping so a 0.03-inch thick, quarter-inch diameter, hole was left. This half-inch diameter section was 0.78 inches long. The plug was filed flush to the inside curve of the 1.5-inch pipe.

The resonator cavity body was then threaded into the larger inside diameter of the branch, where female threads where machined. Two pieces of 1.5-inch, schedule 80, stainless steel pipe were welded onto each end of the T-fitting. Two 1.5-inch, 1500 pound, stainless steel, weld neck flanges were each welded onto the end of each piece of pipe. As mentioned, the motor was attached to one flange, and a second pipe and flange section, 12.5 inches upstream, was attached to the other flange.

An eighth-inch diameter Endevco dynamic pressure transducer was attached 2.5 inches aft of the entrance plane of the motor, 12.16 inches downstream from the resonator cavity centerline. (Refer to List of Equipment placed with the Tables, Figures & Symbols section.) The transducer was intended to measure any disturbances caused by the Helmholtz resonator at this point in the flow.

Two static pressure probes were also attached to the system. One was threaded into a hole in the motor casing that was drilled 4.5 inches forward of the motor's exit plane. The other was installed 17.34 inches upstream of the Helmholtz resonator, in a 1.5-inch diameter pipe, ahead of the upstream flange. On the other side of the test bay wall two 0 - 300 psig dial pressure gauges were each connected, via heavy duty, quarter-inch diameter, copper tubing, to one of the two static probes. (Refer to Figure 3.4.)

B. TESTS

High pressure air (up to 200 psig) was allowed to flow through the foregoing apparatus. The resonator frequency was measured using an HP 3582A Spectrum Analyzer, which was connected to the transducer by way of a B & K, Type 2112, Audio Frequency Spectrometer. Several parts of the set up were changed for each set of tests, i.e., the motor was removed, the microphone was attached to the aft end of 1.5-inch pipe; the motor was replaced, but without its fuel grain; injector and fuel grain were removed; the exit nozzle was removed from motor, with the fuel grain replaced, but with no injector. Finally, the dynamic pressure transducer was replaced with a quarter-inch diameter B & K microphone after the former was damaged, causing it to produce obviously erroneous readings.

For one set of tests the exit nozzle was removed, leaving a one-inch exit diameter. The injector was also left out but the 18-inch plexiglass was installed inside the motor casing.

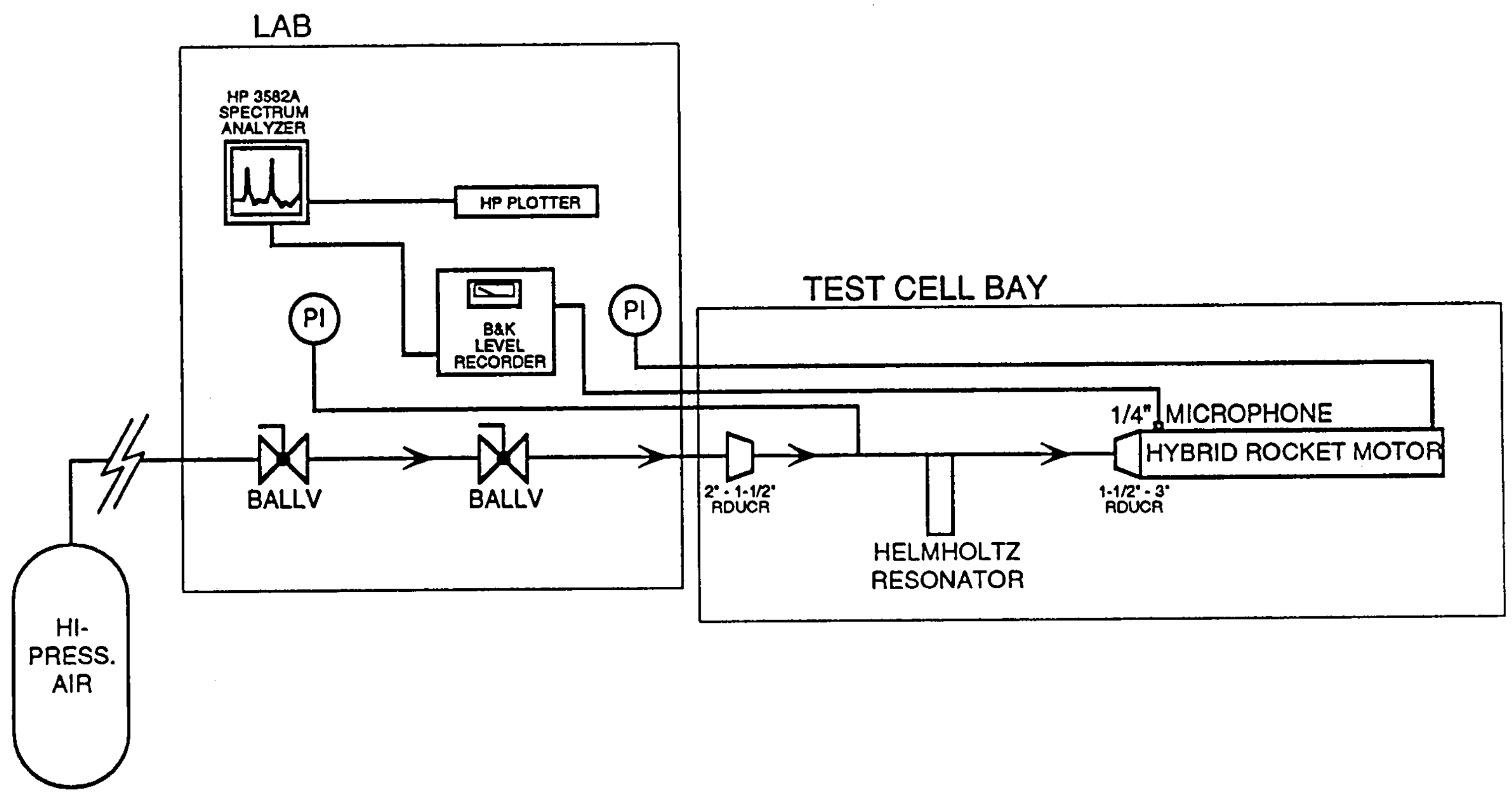

Figure 3.4 Stainless Steel Apparatus With Transducer, Then Microphone, In Combustion Chamber Casing

A hole was drilled though the wall of the T-fitting that connected the resonator to the 1.5-inch pipe, 180 degrees from, and in the same cross-sectional plane, as the resonator aperture. The microphone was installed into this hole, taking care to keep it flush with the inside wall of the pipe. (Refer to Figure 3.5.) Tests were performed with resonator cavity lengths varying from 2.85 to 6.10 inches. These lengths include an adjustment made to account for the 0.5-inch diameter section cut into the aft end of the Teflon-copper plug.

C. REVISED APPARATUS

The stainless steel 1.5-inch pipe and T-fitting the resonator was attached to was replaced with a 1.5-inch diameter, schedule 80, PVC pipe and T-fitting. (Refer to Figure 3.6.) This was done to see if some of the measured disturbances were caused by the discontinuity at stainless steel flange connections. The PVC pipe was cut so that the center line of the resonator was 15.5 inches upstream from the forward cross-sectional plane of the motor's entrance flange. The motor was installed. The transducer was replaced by the microphone, still at the precombustion chamber. The flanges that were upstream of the resonator were not replaced, including the section with the forward static probe. Instead, male threads were machined into the forward end of the PVC pipe, and then it was threaded into the two-inch diameter, high-pressure inlet pipe through a 2- to 1.5-inch reducer. The aft static pressure probe remained in place on the post-combustion section of the motor.

The geometry of the resonator was also changed. There was much difficulty in turning the Teflon-copper plug to where it would be exactly flush with the inner pipe wall. When it was flush, it would turn when the resonator cavity was threaded in behind it. It was much too difficult to tell when turning of the

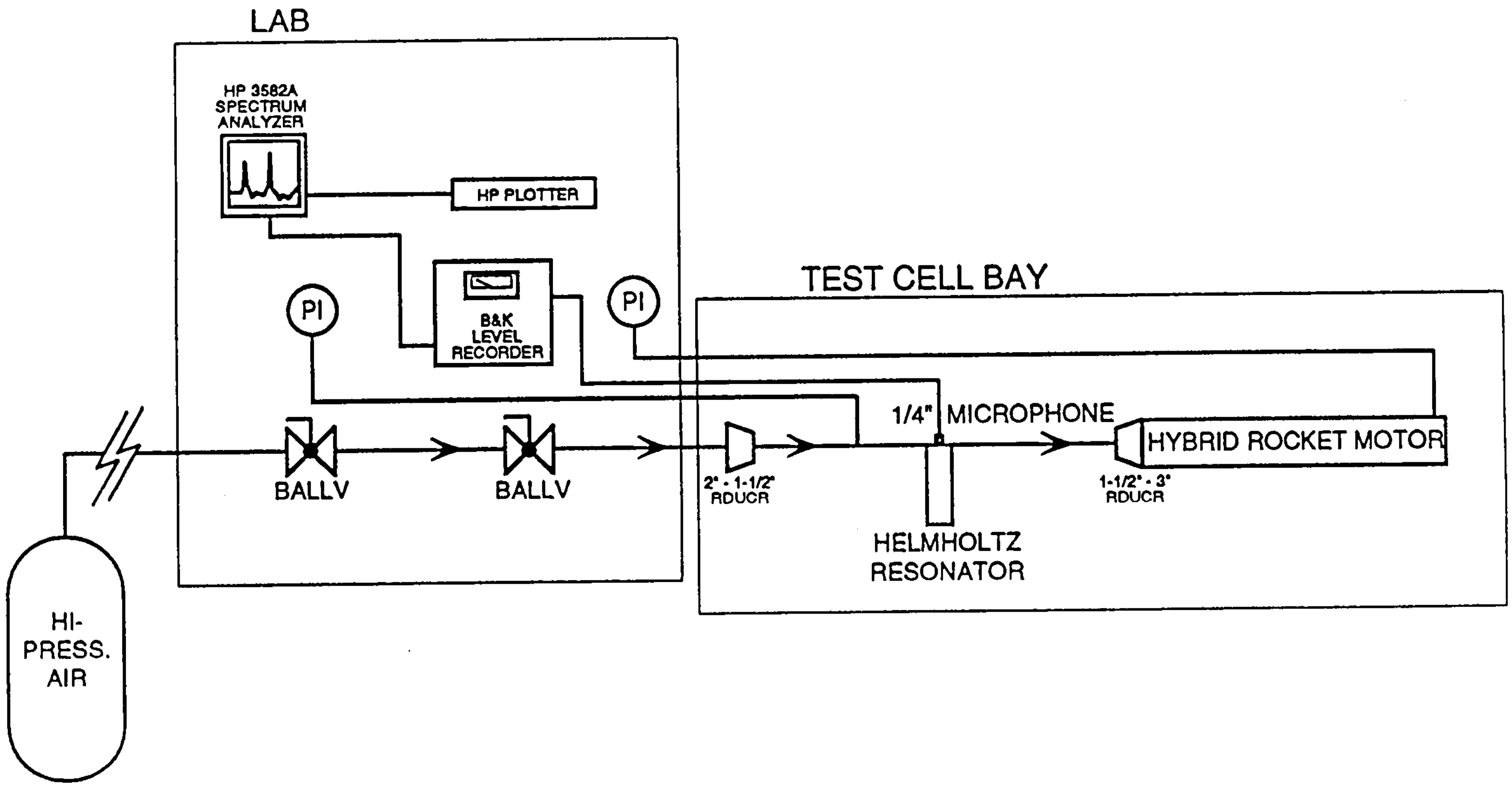

Figure 3.5 Microphone Installed In Stainless Steel Apparatus Straight Across From Helmholtz Resonator

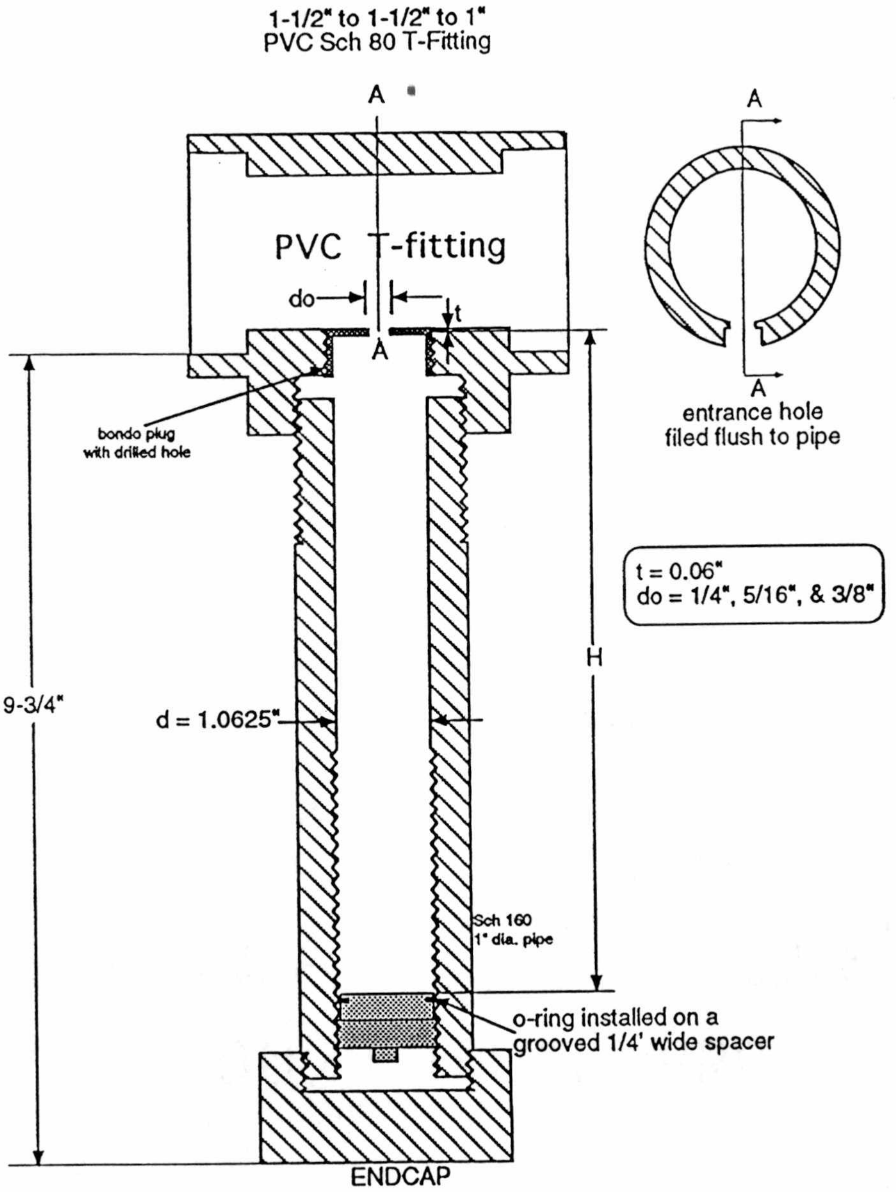

Figure 3.6 Helmholtz Resonator
Attached To Sch 80, PVC T-Fitting

cavity body should be stopped. Arrows etched on the T and cavity body did not work, since the body never started turning the plug at the same point each time. Without a flush plug, the frequency readings were drowned out by the noise due to the protruding plug. Therefore, the plug was replaced with Bondo, a type of resin that would harden completely in about a half hour when it was mixed with a hardener. (Refer to Figure 3.7.) The hardened bondo, in the plug hole, was filed down so that it was flush with the inner pipe wall. After complete hardening a quarter-inch hole was drilled through the centerline of the bondo. With a flat-end drill, a one-inch diameter hole was drilled into the bondo so that the aperture was 0.06 inches thick. Care was taken, since bondo chips easily. Note that there is no longer a step between the aperture and the cavity diameters as there was before (refer to Figure 3.3). Again, frequency measurements were made using the microphone in conjunction with the Spectrum Analyzer and the Audio Frequency Spectrometer. The cavity length was varied between 2.5 and 5.75 inches. Resonant frequency peaks were noted both inside and outside the resonator cavity.

D. APPARATUS ADJUSTMENTS AND DATA ACQUISITION

An HP 7035B, X-Y Recorder was connected to the Spectrum Analyzer to record the measure spectra. With the hybrid motor installed, but without the exit nozzle nor injector, seven tests were made and plotted, varying the cavity length between 2.5 and 8.75 inches. Noted peaks were recorded, by hand, from the spectrum analyzer screen onto the plot itself. These plots were labeled RECORD's #1 - 7 in numerical order of occurrence. Data on geometry and set-up was noted on the back of each plot.

Following the above tests, the hybrid motor was removed. The blank

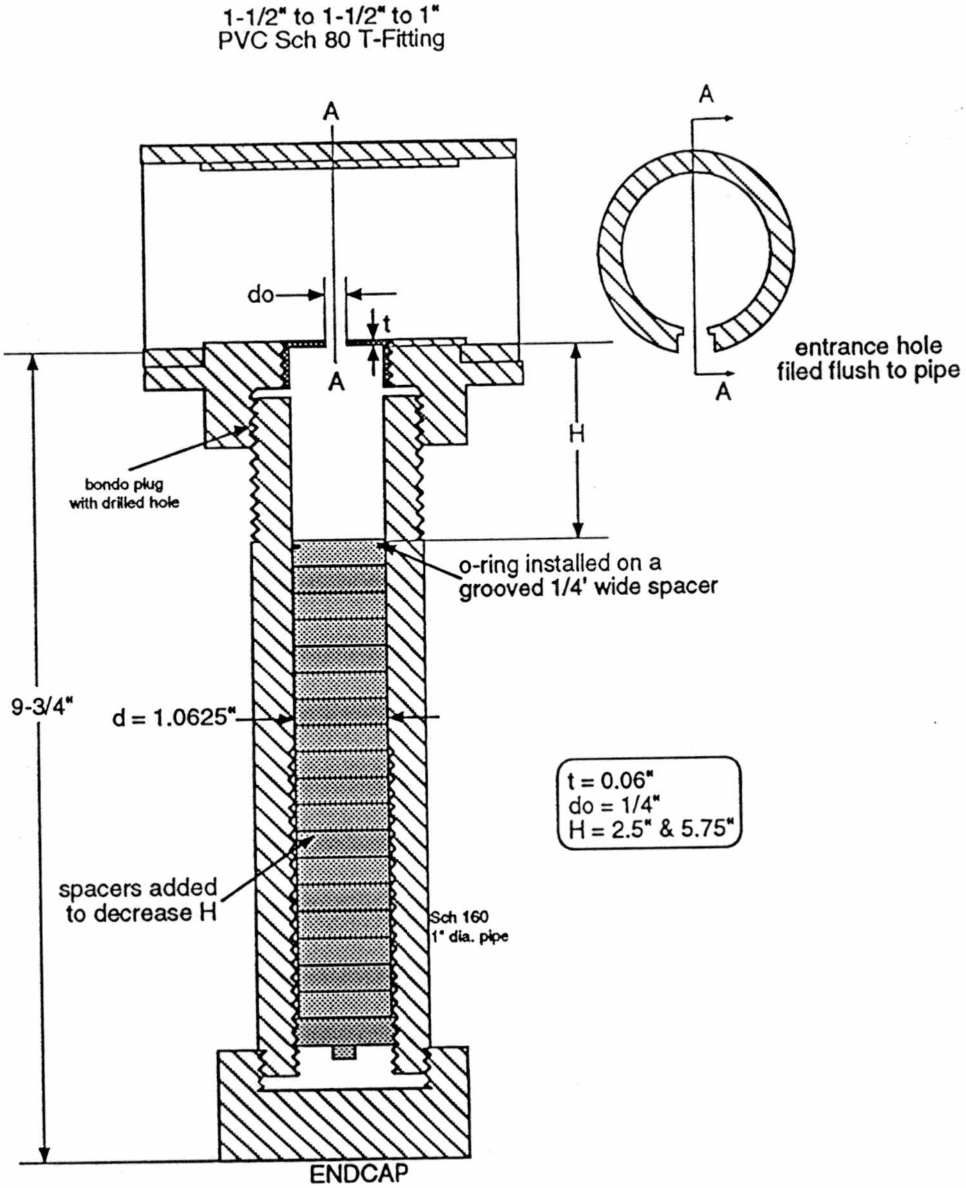

Figure 3.7 Helmholtz Resonator Aperture Made Of Bondo

flange, without the exit nozzle installed, was bolted to the aft flange of the 1.5-inch PVC pipe flange. (Refer to Figure 3.8.) The quarter-inch aperture was drilled to a 0.31-inch diameter. Frequency measurements were again taken and plotted at various cavity lengths. Then, the aperture was drilled to 0.38 inches in diameter. More measurements were made at various cavity lengths.

A 0.04-inch inner diameter, 0.06-inch outer diameter, tube was used to construct a pitot probe and a static probe. The pitot probe was then installed, through the hole made for the microphone in the 1.5-inch pipe, across from the resonator opening. It was made long enough to measure pressure in the centerline of the flow. The section of this probe parallel to the centerline was 1.40 inches long. A second hole was drilled 3.25 inches upstream of the pitot probe entry point, where the static probe was installed. (Refer to Figure 3.9.) Care was taken to keep this probe out of the flow completely. Like the previous pressure probes, these were also connected to dial gauges through copper tubing, although more precise dial gauges were used in place of the 0 - 300 psig dial gauges originally used. This time, two Wallace & Tiernan gauges were used. One gauge measured in inches of water, while the other measured in psig. The former had a scale of 0 - 129 inches H_2O-gauge, while the later, 0 - 4.3 psig. The zero pressure on the former was +0.15 in H_2O, and –0.005 psi for the latter. Measurements were taken, with the blank flange, with the nozzle still installed in it, 15.5 inches downstream of the Helmholtz resonator centerline and velocity was calculated. The inlet pressure that was measured 35.5 feet upstream was used as a reference, assuming P_t would remain constant with P_s, since the pitot tube had to be removed in order to measure frequency with the microphone through the same hole. Note that the static probe was left in its initial location at all times. (Refer to Figure 3.10.) Separate pressure

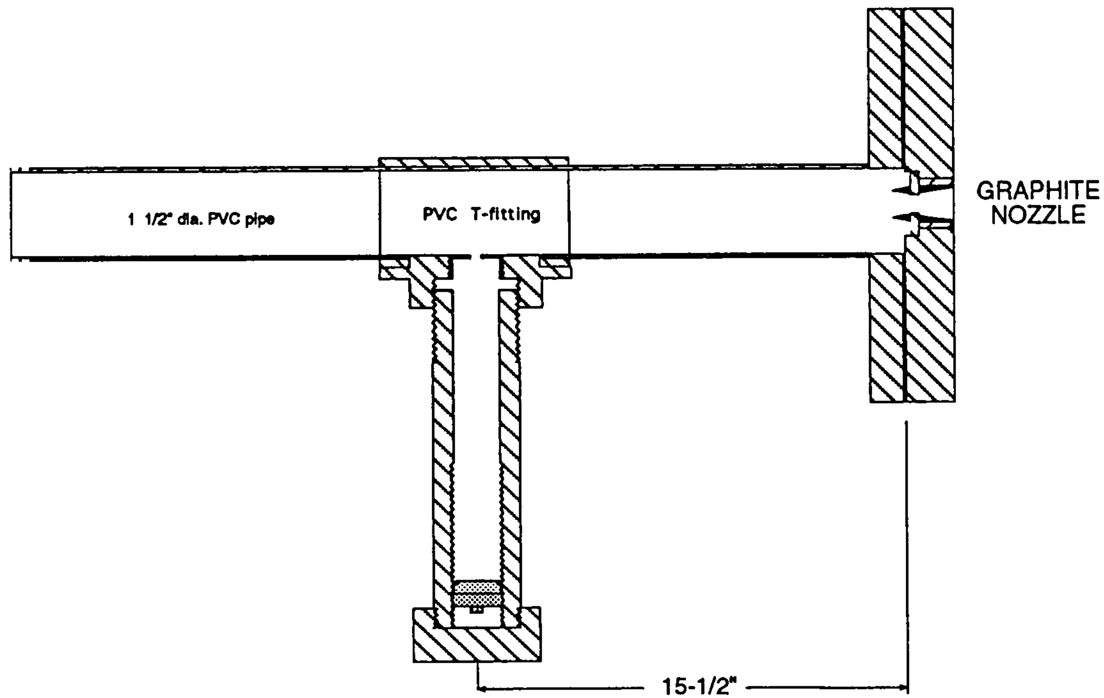

Figure 3.8 Blank Flange, With Nozzle, Installed Downstream Of The Resonator

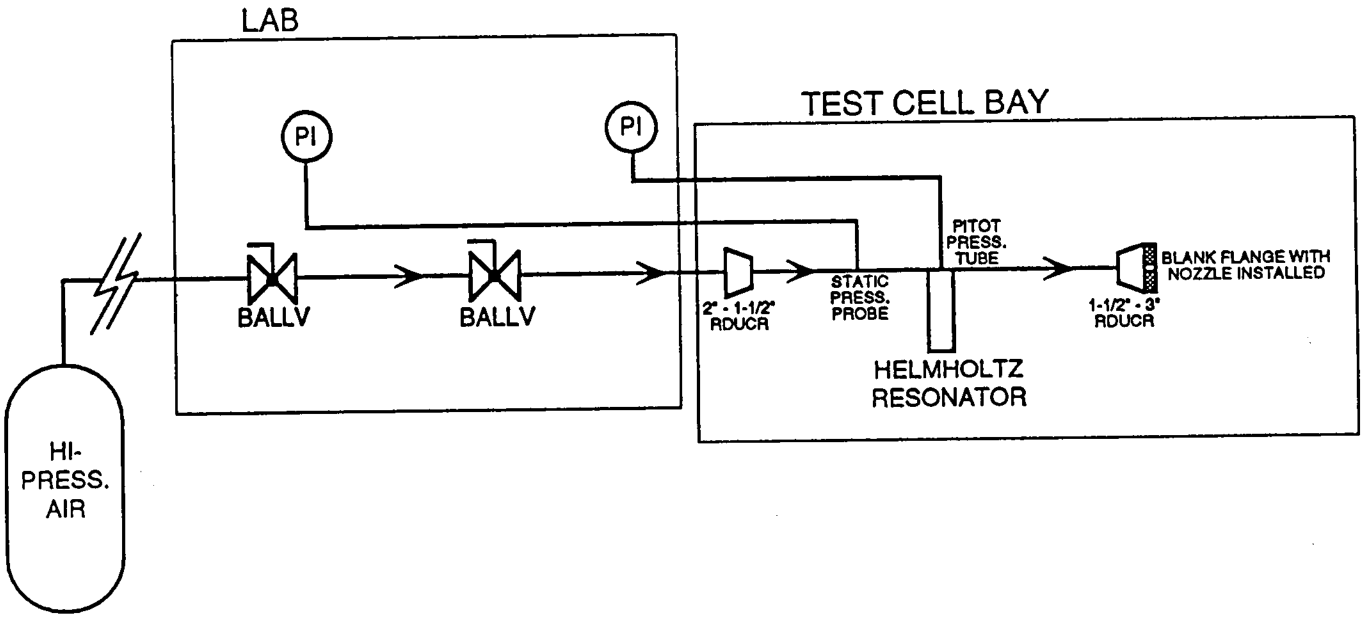

Figure 3.9 Static & Total Pressure Probes Installed In PVC Apparatus

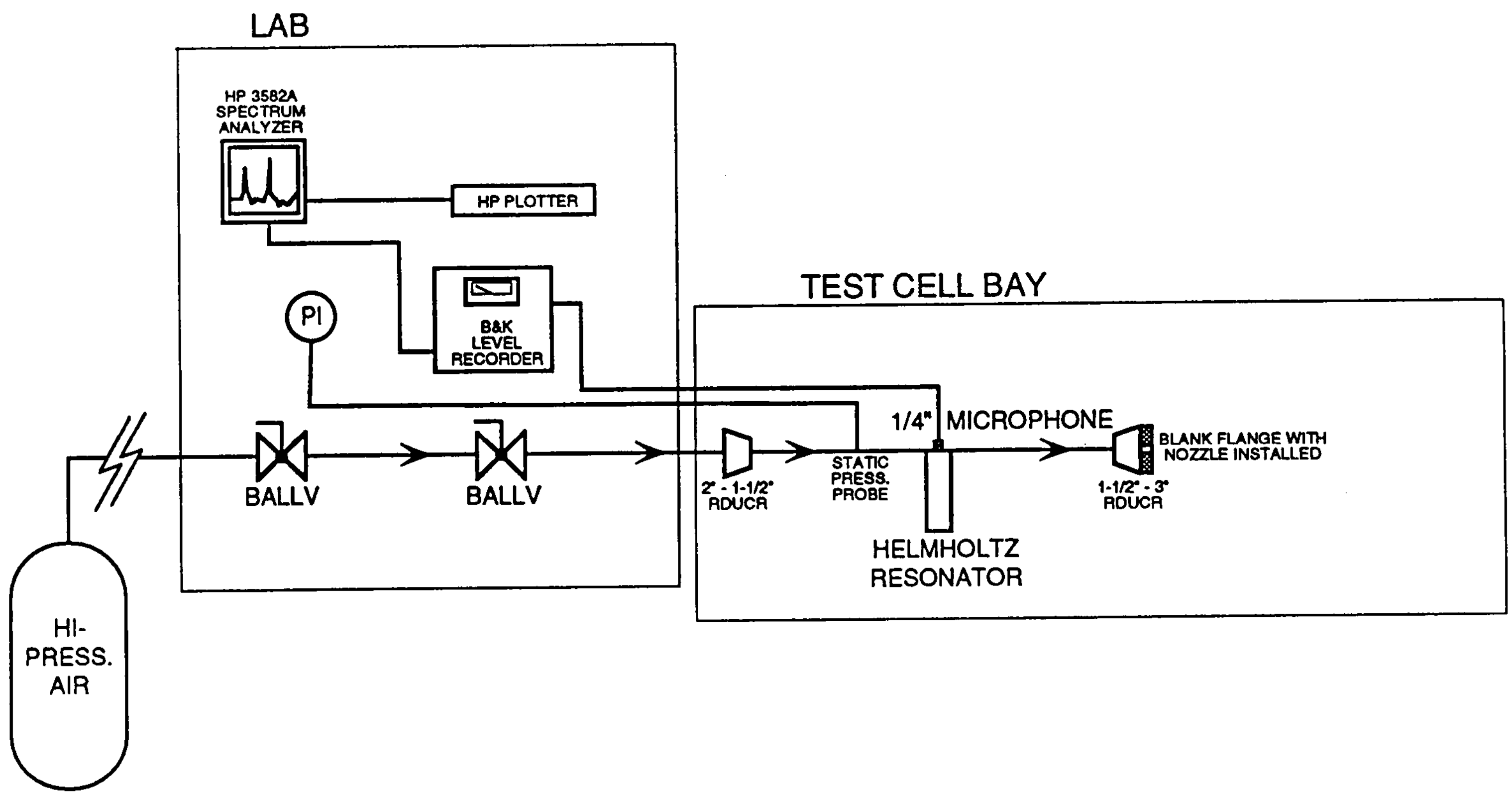

Figure 3.10 Static Pressure Probe & Microphone Installed In PVC Apparatus

measurements were made using the Wallace & Tiernan gauges at the several different velocities. These two gauges caused too much error in the velocity calculations, hence the inches of water gauge was removed, and both the static and total pressure lines were connected to the psig gauge to measure the pressure differential.

The pitot tube was replaced with the microphone and several measurements were made, varying the velocity each time, for a 2- and a 2.5-inch cavity length. The aperture was still 0.38 inches in diameter, and its thickness 0.06 inches. Note that the diameter of the cavity was never changed: it always remained at 1.06 inches.

The aperture hole was changed, employing the easy-to-use bondo to a quarter-inch diameter hole, with a thickness of a quarter-inch. A hole was drilled through the center of the endcap. The endcap screwed onto the end of the cavity body. The same microphone was moved from the outside of the Helmholtz resonator to inside its cavity through the endcap hole. (Refer to Figures 3.11, 3.12 & 3.13.) The hole in the 1.5-inch line was plugged. Care was taken not to allow the plug to protrude into the airflow inside the line. Since there was not an easy way to use the spacers, for changing the cavity length in conjunction with the microphone, three more resonator cavity bodies were machined to varying lengths and threaded like the original one. These resonator cavities were constructed from the same piping as the original one. The cavity lengths were 3.25, 4.63, 7.25 and 9.25 inches. The inner diameter of the endcap was 1.77 inches. Since none of the resonator cavities could ever be threaded far enough into the endcap to be flush against it, a spacer 1.06 inches in diameter and 0.78 inches thick, was constructed and installed into that open space. Hence, the cavity length, for each cavity body, was kept constant

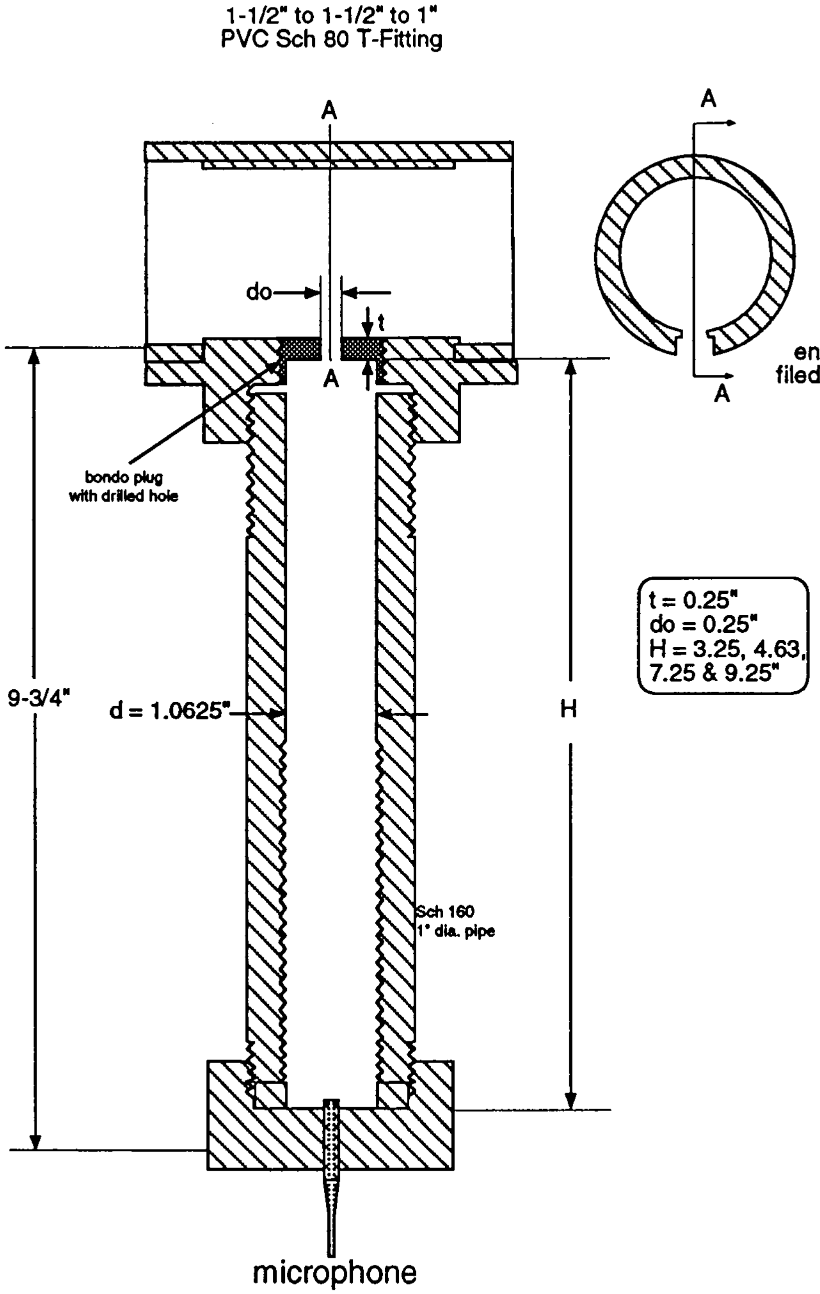

Figure 3.11 Microphone Installed
In Aft End Of Helmholtz Resonator

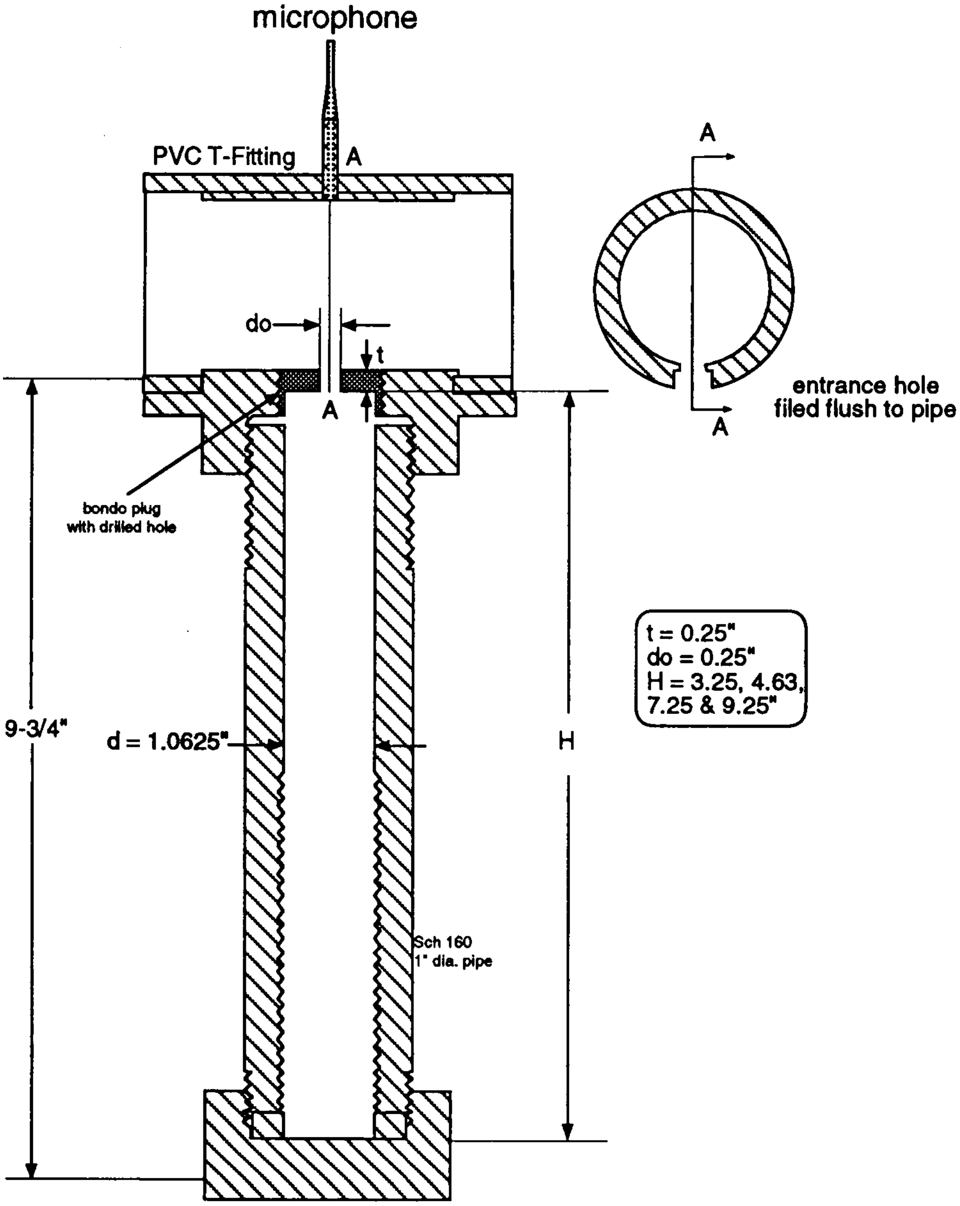

Figure 3.12 Microphone Installed Across From Helmholtz Resonator

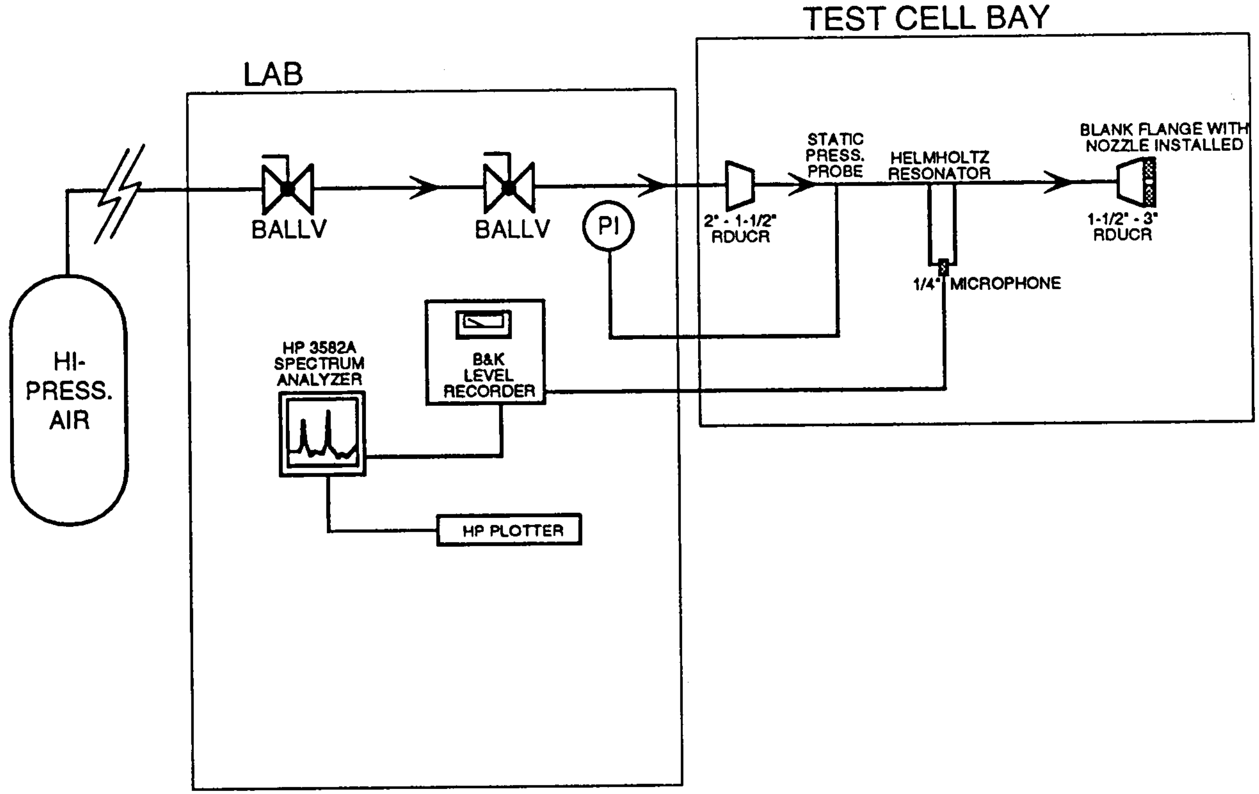

Figure 3.13 System With Microphone Positioned Inside Helmholtz Resonator

at 1.06 inches for the entire length. Tests of two different cavity lengths were made, and their respective frequencies were plotted.

The aperture was drilled to 0.31 inches in diameter, and two tests, using two different cavity lengths, were made and their respective frequencies plotted.

The apparatus was removed from the main, two-inch diameter, air line and the inner wall of the 2- to 1.5-inch reducer was smoothed out using bondo. Then the apparatus was reinstalled. Tests were then made at two different cavity lengths and their respective frequencies were plotted.

The cavity body was removed and the aperture was refilled with bondo. The diameter of the aperture was drilled to 0.31 inches, with a thickness of 1.31 inches. (Refer to Figure 3.14.) Tests were made at two different cavity lengths and the frequencies for each were plotted.

The aperture was then drilled to a quarter-inch diameter, holding the thickness at 1.33 inches. Tests were made at two different cavity lengths, plotting each of their frequencies.

The aperture was again drilled, this time to a 0.38-inch diameter, still keeping the thickness at 1.33 inches. Tests at varying velocities for each of the four cavities were completed and their frequencies plotted. This set of plots was labeled RECORD's #21 - 34.

The position of the microphone was changed from the inside of the cavity back to the outside of it, in the same hole as before, in the 1.5-inch line above the aperture. Tests at varying velocities, for all four cavities were again completed and their frequencies were plotted. Then more plots of the frequency inside the cavity were also made. This set of plots was recorded and labeled RECORD's #35 - 38.

The aperture diameter was increased to 0.44 inches in diameter. Tests

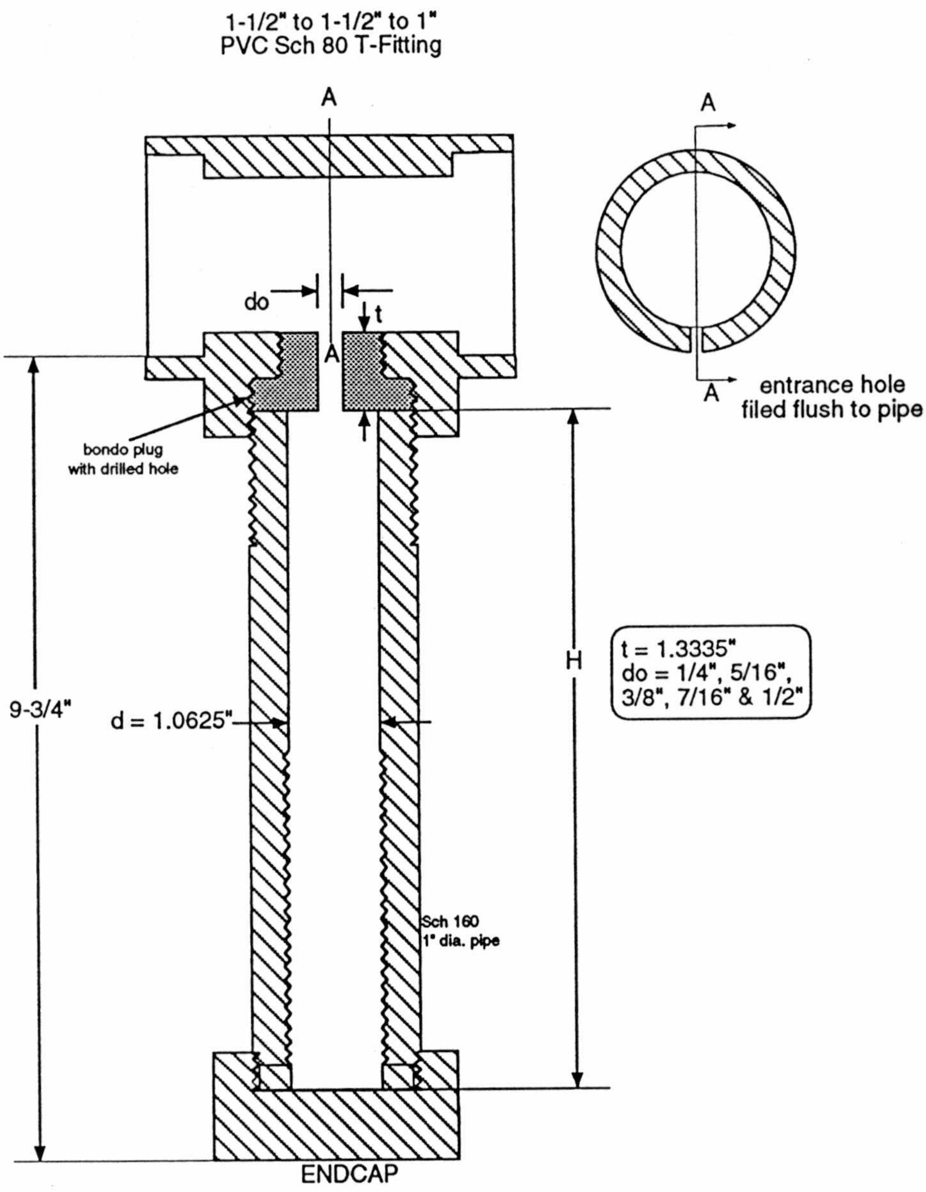

Figure 3.14 Helmholtz Resonator
With Change In Aperture Thickness

were made and their respective frequencies plotted for different velocities and cavity lengths. These were labeled RECORD's #39 - 52.

The aperture was drilled, for the final time, to a half-inch diameter. Its thickness has not been changed from 1.33 inches. Several more tests, of varying velocities, were made and plotted like before. These were labeled RECORD's #53 - 60.

Velocities were then rechecked by reinstalling the pitot tube in the same hole it was previously in. It was found that the human error in reading the two gauges, one in inches of water, the other in psi, unacceptable. Therefore, the two probes were connected into the psi gauge and the differential was read directly from the gauge.

The exit nozzle was removed from the blank flange allowing the high pressure flow to exit through the one-inch hole. The pressure differential was again recorded at various upstream pressure settings.

Several more tests were made and their respective frequencies recorded. These were labeled RECORD's #61 - 73. These were done using the 7.25- and 9.25-inch length cavities, each at the three velocities: 56, 96, and 143 ft/s. One frequency spectra was measured with the microphone inside and the other outside the cavity.

RECORD's #74 & 75 are the microphone calibration curves. The microphone was placed inside a calibrator. The calibrator emitted a 1000 Hz pure tone. It was a 114 dB signal.

The final three tests, RECORD's #76 - 78, were done without a cavity. Rather, an endcap was fabricated that threaded flush against the aperture, where $d = H = 0$.

The spectrum analyzer was checked from a signal generator output of different known frequencies and amplitude to ensure its readings were accurate. They were.

CHAPTER IV

RESULTS & DISCUSSION

A. PREVIEW

The purpose of this experiment was to design a Helmholtz resonator that would produce predetermined resonant frequencies with enough power to increase the combustion turbulent mixing, hence the fuel burn rate, in a hybrid rocket motor. To achieve this, the resonator was placed upstream of the hybrid rocket motor. Included in the motor was an injector, a solid fuel section, and an exit nozzle. A reduced-scale version of a hybrid rocket motor was designed and fabricated using plexiglass for the fuel, and gaseous oxygen for the oxidizer. The gaseous oxygen would be introduced into the hybrid at up to approximately 800 psi. (Refer to Appendix 1.)

Considering limitations of piping, reducers and flanges, the resonator was placed as closed as possible to the hybrid motor. Before any time and money was invested in studying how the resonator affected the hybrid rocket motor flow, cold flow tests were performed and are described in this thesis. Performing cold flow tests allowed an inexpensive way to perfect the resonator so it would have the greatest effect on the motor. As described in Chapter 2, several of the tests included the motor, but most did not. Choked and unchoked flow tests were performed, both with and without the motor. The microphone was first placed in the precombustion chamber to determine if the resonator had a measurable affect on the flow within the engine. (Refer to Appendix 2 for the distortion and directional characteristics and the dynamic range of the microphone used, and the microphone calibration curve made using the HP Spectrum Analyzer).

During the tests several adjustments were made to the geometry of the original resonator in order to find the best geometry that would most effect the hybrid rocket motor flow. All revised geometries were based on the resonator equations developed by Panton (Panton, 1990). (Refer to Equations (2.13) & (2.14).) Panton demonstrated that the maximum nondimensional cavity pressure,

$$\left[\frac{P'_{rms}}{q}\right]_{max}$$

occurred when the nondimensional freestream velocity was equal to:

$$\frac{1}{Str} = \frac{U}{d_o f_o} = 3.75 \qquad (4.1)$$

where Str is the Strouhal number, P'_{rms} is the pressure in the cavity measured by the microphone, and q is the dynamic pressure of the freestream velocity. From the data given in Panton, 1990, $[P'_{rms}]_{max}$ = 6.06 lb/ft^2 and f_o = 645 Hz. (U = 55 mph, , d_o = 0.0338 ft, H = 0.3501 ft, and c = 1116 ft/s and ρ = 0.002328 slugs/ft^3 are assumed).

In the present tests the air moved over the aperture at a velocity between 5 and 143 ft/s. Assuming a critical Reynolds number, Re_{crit}, of 2100 for pipe flow (Vennard, 1954), all the flows were turbulent. Table IV.i indicates the Reynolds number, Re, for each velocity.

$$Re = \frac{\rho_{air}\, U\, D_p}{\mu_{air}} = 789.12\ U$$

TABLE IV.i REYNOLD'S NUMBER

U ft/s	Re
2.66	2,099
55	43,402
56	44,191
96	75,756
143	112,845

$\rho_{air} = 2.38 \times 10^{-3}$ $lb_f\ s^2/ft^4$
$m_{air} = 3.77 \times 10^{-7}$ $lb_f\ s/ft^2$
$\nu_{air} = 1.58 \times 10^{-4}$ ft^2/s
$D_{pipe} = 1.5$ in
$Re_{crit} = 2100$ (Vennard, 1954)
$U_{crit} = 2.7$ ft/s

B. TEST SUMMARY

Tables IV.ii & IV.iii indicate the configurations of the tests performed for this experiment. The data summarized in Table IV.iii was plotted using the HP X-Y Plotter in conjunction with the HP Spectrum Analyzer (refer to List of Equipment) while the data summarized in Table IV.ii was not.

The data is listed in Table IV.ii in the order in which it was obtained and is numbered in the first column. The following four columns list the Helmholtz resonator geometry incorporated for each. An "x" found in one of the next three columns describes where the microphone was positioned during the test: either in the precombustion chamber casing of the motor, m, in the oxidizer line, ol, or in the aft end of the Helmholtz resonator, Hr. The following nine columns describe the details of each test set up with x's in the appropriate columns. If

TABLE IV.ii DATA FOR TESTS #1 - 24

#	d	do	t	H	FMP			INSTALLED								R:M	P1	P2	NOTES
	in	in	in	in	m	ol	Hr	m	i	pg	n	Tc	bon	SS	PVC		psig	psig	
1	1.06	0.25	0.03	6.10	x			x	x	x	x	x		x					•multiples of 60 Hz
2	1.06	0.25	0.03	6.10	x			x	x	x	x	x		x					•peak @ 5000 Hz
3	1.06	0.25	0.03	3.87	x			x	x	x	x	x		x					
4	1.06	0.25	0.03	4.10	x			x	x	x	x	x		x			75		•1250 Hz peak due to offset aperture plug
5	1.06	0.25	0.03	4.10	x			x	x	x	x	x		x			50		•1250 Hz peak due to offset aperture plug
6	1.06	0.25	0.03	2.85	x			x	x	x	x	x		x					•1250 Hz peak due to offset aperture plug
7	1.06	0.25	0.03	0.10	x			x	x	x	x	x		x			50		•1250 Hz peak due to offset aperture plug
8	1.06	0.25	0.03	0.10	x			x	x	x	x	x		x			100		•1250 Hz peak due to offset aperture plug
9	1.06	0.25	0.03	2.98	x			x	x	x	x	x		x			50		•1250 Hz peak due to offset aperture plug
10	1.06	0.25	0.03	2.98	x			x	x	x	x	x		x			100		•1250 Hz peak due to offset aperture plug
11	1.06	0.25	0.03	2.85	x			x		x	x	x		x		80 0	80		•nearly uniform amplitude
12	1.06	0.25	0.03	2.85	x			x		x	x	x		x		80 0	150		•nearly uniform amplitude
13	1.06	0.25	0.03	2.85	x			x		x	x	x		x		80 0	45		•nearly uniform amplitude
14	1.06	0.25	0.03	5.25		x		x		x		x		x		80 0	0	0	•freq and SPL values inTable IV.v
15	1.06	0.25	0.03	5.25		x		x		x		x		x		80 0	0	0	•freq and SPL values inTable IV.v
16	1.06	0.25	0.03	5.25		x		x		x		x		x		80 0	5	0	•freq and SPL values inTable IV.v
17	1.06	0.25	0.03	5.25		x		x		x		x		x		80 0	10	0	•freq and SPL values inTable IV.v
18	1.06	0.25	0.06	5.25		x		x		x		x		x		80 0	0	0	•freq and SPL values inTable IV.v
19	1.06	0.25	0.06	4.25		x		x		x		x		x		80 0	10	0	•freq and SPL values inTable IV.v
20	1.06	0.25	0.06	4.25		x		x		x		x		x		80 0	0	0	•freq and SPL values inTable IV.v
21	1.06	0.25	0.06	4.50	x			x					x		x	60 20			•multiples of 60 Hz
22	1.06	0.25	0.06	4.00	x			x					x		x	60 20			•amplitudes of the background
23	1.06	0.25	0.06	5.75	x			x					x		x	60 20			•amplitudes of the background
24	1.06	0.25	0.06	4.50	x			x					x		x	60 20			•amplitudes of the background

NOTE: SHADED AREAS-NO MEASUREMENTS TAKEN

m- motor
ol-oxidizer line
Hr-resonator
i-injector
pg-plexiglass
bon-bondo
FMP-frequency measuring pt
n-nozzle
pg-plexiglass
Tc-Teflon copper plug
SS-stainless steel
R:M-range:multiplier

TABLE IV.iii DATA FOR PLOTTED TESTS (BONDO APERTURE, PVC SET UP)

RECORD	d	do	t	H	FMT			INSTALLED					P2	Pt	Ps	delta P	NOTES
#	in	in	in	in	m	ol	Hr	m	i	pg	n	R:M	psf	in H20	psf	psi	
1	1.06	0.25	0.06	4.50	x			x					100				
2	1.06	0.25	0.06	4.50	x			x					200				
3	1.06	0.25	0.06	4.50	x			x					400				
4	1.06	0.25	0.06	2.50	x			x					100				
5	1.06	0.25	0.06	2.50	x			x					200				
6	1.06	0.25	0.06	2.50	x			x					400				
7	1.06	0.25	0.06	8.75	x			x					100				
8	1.06	0.25	0.06	6.50		x											
9	1.06	0.38	0.06	4.75		x											•new peak noted at 1810 Hz
10	1.06	0.38	0.06	2.50		x					x			19.2	100		
11	1.06	0.38	0.06	2.50		x					x			38.0	200		
12	1.06	0.38	0.06	2.50		x					x			56.3	300		
13	1.06	0.38	0.06	2.50		x					x			74.6	400		
14	1.06	0.38	0.06	2.50		x					x			93.4	500		
15	1.06	0.38	0.06	2.50		x					x			112.2	600		
16	1.06	0.38	0.06	2.00		x					x			19.2	100		
17	1.06	0.38	0.06	2.00		x					x			38.0	200		
18	1.06	0.38	0.06	2.00		x					x			56.3	300		
19	1.06	0.25	0.25	4.63			x				x			112.2	600		
20	1.06	0.38	0.25	4.63			x				x			19.2	100		•smoothed 1.5-2" reducer 1st
21	1.06	0.38	1.33	7.25			x				x				50		
22	1.06	0.38	1.33	7.25			x				x			112.2	600		•observed pk in cavity
23	1.06	0.38	1.33	7.25			x				x						•observed pk in cavity
24	1.06	0.38	1.33	7.25			x				x						•observed pk in cavity
25	1.06	0.38	1.33	9.25			x				x						•pk observed different for this H
26	1.06	0.38	1.33	9.25			x				x						•observed pk in cavity
27	1.06	0.38	1.33	9.25			x				x						•observed pk in cavity
28	1.06	0.38	1.33	9.25			x				x						•observed pk in cavity
29	1.06	0.38	1.33	9.25			x				x						•observed pk in cavity
30	1.06	0.38	1.33	9.25			x				x				550		
31	1.06	0.38	1.33	4.63			x				x				700		
32	1.06	0.38	1.33	4.63			x				x				800		
33	1.06	0.38	1.33	3.25			x				x				700		
34	1.06	0.38	1.33	3.25			x				x				600		
35	1.06	0.44	1.33	9.25		x					x				200		

TABLE IV.iii (continued)

RECORD	d	do	t	H	FMT			INSTALLED					P2	Pt	Ps	delta P	NOTES
#	in	in	in	in	m	ol	Hr	m	i	pg	n	R:M	psf	in H20	psf	psi	
36	1.06	0.44	1.33	9.25			x				x				500		
37	1.06	0.44	1.33	9.25		x					x				700		
38	1.06	0.44	1.33	7.25		x					x				600		
39	1.06	0.44	1.33	9.25			x				x				350		
40	1.06	0.44	1.33	9.25			x				x				400		
41	1.06	0.44	1.33	9.25		x					x				350		
42	1.06	0.44	1.33	9.25		x					x				400		
43	1.06	0.44	1.33	7.25			x				x				600		
44	1.06	0.44	1.33	7.25		x					x				400		
45	1.06	0.44	1.33	7.25		x					x				600		
46	1.06	0.44	1.33	4.63			x				x				1050		
47	1.06	0.44	1.33	4.63			x				x				900		
48	1.06	0.44	1.33	4.63		x					x				900		
49	1.06	0.44	1.33	4.63		x					x				1050		
50	1.06	0.44	1.33	3.25			x				x				0		
51	1.06	0.44	1.33	3.25			x				x				1000		
52	1.06	0.44	1.33	3.25			x				x				950		•noise only
53	1.06	0.50	1.33	9.25			x				x				400		•noise only
54	1.06	0.50	1.33	9.25			x				x				300		
55	1.06	0.50	1.33	9.25		x					x				300		
56	1.06	0.50	1.33	9.25			x				x				400		
57	1.06	0.50	1.33	7.25			x				x				600		
58	1.06	0.50	1.33	7.25			x				x				700		
59	1.06	0.50	1.33	7.25		x					x				600		
60	1.06	0.50	1.33	7.25		x					x				700		
61	1.06	0.50	1.33	9.25			x										
62	1.06	0.50	1.33	7.25			x								100	0.160	
63	1.06	0.50	1.33	7.25			x								10	0.015	
64	1.06	0.50	1.33	7.25			x								50	0.070	
65	1.06	0.50	1.33	7.25		x									10	0.015	
66	1.06	0.50	1.33	7.25		x									50	0.070	
67	1.06	0.50	1.33	7.25		x									100	0.160	
68	1.06	0.50	1.33	9.25		x									10	0.015	
69	1.06	0.50	1.33	9.25		x									50	0.070	
70	1.06	0.50	1.33	9.25		x									100	0.160	
71	1.06	0.50	1.33	9.25			x								10	0.015	

TABLE IV.iii (continued)

RECORD	d	do	t	H	FMP			INSTALLED					P2	Pt	Ps	delta P	NOTES
#	in	in	in	in	m	ol	Hr	m	i	pg	n	R:M	psf	in H20	psf	psi	
72	1.06	0.50	1.33	9.25			x					80:-10			50	0.070	
73	1.06	0.50	1.33	9.25			x					80:-10			100	0.160	
74												60:-10					•mic calibration: 114dB, 1000Hz
75												60:-10					•mic calibration: 114dB, 1000Hz
76	1.06	0.50	1.33	0.00			x								10	0.015	
77	1.06	0.50	1.33	0.00			x								50	0.070	
78	1.06	0.50	1.33	0.00			x								100	0.160	

m- motor
ol-oxidizer line
Hr-resonator
i-injector
pg-plexiglass
bon-bondo
FMP-frequency measuring pt
n-nozzle
pg-plexiglass
Tc-Teflon copper plug
SS-stainless steel
R:M-range:multiplier

NOTE: SHADED AREAS-NO MEASUREMENTS TAKEN the hybrid motor was installed an "x" is in the column labeled "m". Likewise if the injector was used, i, the plexiglass fuel grain, pg, and/or the exit nozzle, n; the Teflon-copper or bondo aperture plug, Tc or bon; and the stainless steel or PVC apparatus, SS or PVC. The subsequent column provides the Range:Multiplier value set on the B & K Audio Frequency Spectrometer. The next three columns furnish the particular pressure(s) measured, if any. The final column provides any special notes for several of the tests.

Table IV.iii is similar to Table IV.ii described in the previous paragraph, with a few additions and removals. Each X-Y plot produced was labeled with RECORD #. The indications of the pressures measured are different from Table IV.ii and, since all these tests used the PVC apparatus with a bondo resonator aperture, all reference to the materials has been removed. In the following analysis refer to these tables for details.

C. MICROPHONE PLACED IN PRECOMBUSTION CHAMBER

In the first set of tests no spectra plots were made, but rather the data was recorded by hand in the laboratory notebook. The purpose of these tests was to find the Helmholtz resonator geometry that would generate a measurable effect inside the motor. No frequency peaks were observed with the spectrum analyzer, suggesting that the resonator was not affecting the precombustion chamber flow. The frequency versus sound pressure level, SPL, curves looked more like noise, and any observed peaks did not vary with resonator cavity length, as they should if they had actually been generated by the resonator. However, those peaks that were observed will be described.

In Tests #1 - 3 only multiples of 60 Hz were observed. In Tests #4 - 10 a peak was observed at 1250 Hz. At an inlet static pressure, p_1, between 50 and 100 psig, it stood 12.6 and 13.1 dB above the next highest peaks, respectively. It was assumed that the Teflon-copper plug was not flush with the pipe, since it sometimes turned when the resonator cavity body was threaded onto the T-fitting, and that this was the cause of this disturbance. Once the plug was turned flush frequency peaks at 1250 Hz disappeared. A quick analysis can be performed in order to estimate the height of the protrusion. The Strouhal number, Str, is defined as the inverse nondimensional velocity (that is nondimensional frequency):

$$Str = \frac{f_o h}{U}$$

so that

$$h = \frac{Str\, U}{f_o}$$

The unknowns are the Strouhal number, the freestream velocity in the oxidizer line, and the height of the protrusion, h. For a first approximation Str = 0.25 (Hoerner, 1965). Assuming steady, quasi-one-dimensional flow the freestream velocity in the 1.5-inch pipe is estimated. The nozzle has a throat diameter of 0.26 inches. The apparatus assumes the shape in Figure 4.1 (a). This shape is simplified to a reducer shape by assuming vortices form against the blank flange as illustrated in Figure 4.1 (b). Therefore the actual shape of the oxidizer line-blank flange-nozzle can be assumed to be shaped like a nozzle as shown in Figure 4.1 (c). Continuity is

$$(\rho\, U\, A)_p = (\rho\, U\, A)_t$$

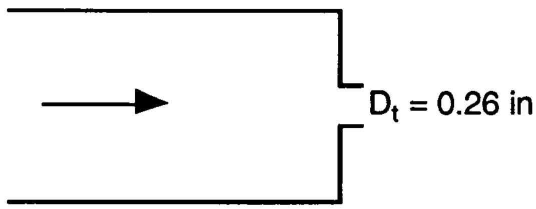

(a) Oxidizer Pipe And Nozzle Configuration

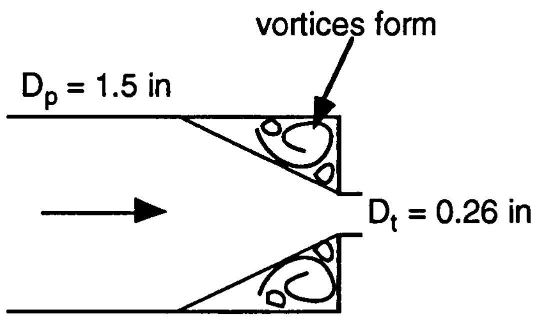

(b) Vortices Form At Blank Flange

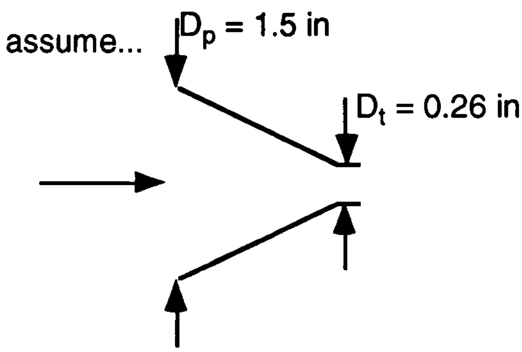

(c) Assumed Shape Of Oxidizer Pipe And Nozzle Configuration

Figure 4.1 Velocity Calculation For Choked Flow where

p - oxidizer pipe

t - nozzle throat.

The velocity is estimated as 55 ft/s, assuming the temperature of the throat is 59 F, and the specific heat ratio, $\gamma = 1.4$. For this velocity the height of the protrusion of the Teflon-copper plug was estimated to be 0.13 inches.

In Tests #11 - 13 only noise was observed with no discernible peaks. The SPL levels were all about equal to those recorded in Test #6, and there was not much change as the inlet line pressure was varied. However, the velocity over the resonator opening was not measured.

Table IV.iv shows the predicted resonant frequencies for the cavity lengths used in this set of tests, but these frequencies were not discernible above the background noise.

D. MICROPHONE PLACED UPSTREAM OF MOTOR

In this set of tests the position of the microphone was moved from the combustion chamber to the 1.5-inch line upstream of the motor. It was installed

TABLE IV.iv ACTUAL DATA WITH PANTON'S FREQUENCY

c ft/s	d_o in	H in	d in	t in	l' in	l in	$(f_o)_t$ Hz
1,117	0.25	2.979	1.0625	0.0313	0.212	1.986	562.5
1,117	0.25	3.686	1.0625	0.0313	0.212	2.263	493.8
1,117	0.25	4.104	1.0625	0.0313	0.212	2.420	461.7
1,117	0.25	6.104	1.0625	0.0313	0.212	3.135	356.4

across from the Helmholtz resonator as described in Chapter III. For these tests the motor remained installed, but the nozzle was removed, leaving a one-inch exit hole. Table IV.v shows the results of tests #14 - 20.

These tables include frequency peaks and their respective SPL's. The heights of these peaks are comparable to the overall noise amplitude. The SPL values were calculated knowing the Range:Multiplier values which were set on the Audio Frequency Spectrometer The SPL value can be determined knowing the SCALE value, and the calibration of the Spectrum Analyzer. SCALE and SPL values are linearly proportional to each other. (The dB reading on the analyzer is referred to as SCALE, to differentiate it from actual SPL values.) For this particular Spectrum Analyzer the following data was determined from the calibration, using a 1000 Hz microphone calibrator, and the Range:Multiplier, R:M, values set on the analyzer.

R : M	SPL dB	SCALE dB
80 : -10	114	-14
60 : 0	114	-4
80 : 0	114	-24

Actual SPL values are based on the scale where 0 dB = 2 x 10^{-5} Pa, i.e.,

$$\text{SPL in dB} = 20 \log_{10}\left(\frac{P'_{rms}}{2 \times 10^{-5}\ \text{Pa}}\right)$$

where,

$$P'^2_{rms} = \overline{P'^2}$$

TABLE IV.v TESTS #14 - 20

H = 5.245 in

Test	P_1 psig	P_2 psig	f Hz	SCALE dB	SPL dB
#9	0	0	260	-24.9	113.1
			400	-25.5	112.5
			650	-27.3	110.7
			800	-24.3	113.7
			950	-24.3	113.7
#10	0	0	396	-24.9	113.1
			648	-28.5	109.5
			724	-30.3	107.7
			852	-26.2	111.8
			880	-29.4	108.6
#11	5	0	100	-25.1	112.9
			260	-21.2	116.8
			400	-22.2	115.8
			480	-23.9	114.1
			650	-22.6	115.4
			790	-20.9	117.1
			950	-21.9	116.1
			1,270	-26.8	111.2
#12	10	0	801	-10.5	127.5
			5,401	-18.1	119.9
			10,701	-10.4	127.6
			16,001	-23.5	114.5
			21,301	-23.2	114.8
#13	0	0	5,401	-27.5	110.5
			10,701	-21.2	116.8
			16,101	-40.3	97.7
			21,401	-42.8	95.2

H = 4.245 in

Test	P_1 psig	P_2 psig	f Hz	SCALE dB	SPL dB
#14	10	0	803	-8.1	129.9
			5,303	-13.5	124.5
			10,703	-11.8	126.2
			16,003	-25.0	113.0
			21,403	-26.1	111.9
#15	0	0	399	highest	
			830	-23.9	114.1
			5,403	-20.7	117.3
			10,803	-13.7	124.3
			16,203	-30.1	107.9
			21,603	-28.4	109.6

CONSTANTS

$d = 1.03125"$
$d_o = 0.25"$
$t = 0.03125"$
$P_{atm} = 14.07$ psia
$T_{atm} = 62.6$ F
Range Multiplier : 80:0

NOTES

- Stainless Steel Set-up
- 1/4" mic. outside res.
- injector removed
- 18" plexiglass installed
- exit nozzle removed
- choked flow

NOTE: All SCALE values were transcribed from the Spectrum Analyzer to the plot by hand.

The overbar denotes the mean value (Dowling & Ffowcs Williams, 1989).

The exit nozzle was not installed for tests #9 - 15 and this indicates that the flows were not choked. Static pressure was measured upstream of the resonator, and downstream, in the aft combustion chamber. However, the stagnation pressure was not measured so the velocity could not be determined. However, it is safe to assume that all three flows were turbulent.

Table IV.vi indicates the resonant frequency that was expected for the two different lengths used in this set of tests. In this table $(f_o)_t$ is the theoretical frequency predicted using equation (2.14) and (2.15). Peaks were not observed at these frequencies above the general background sound level. In some instances peaks were observed at the predicted frequency but they did not change with a change in cavity depth so it was concluded that they were just part of the background noise. Thus, it was concluded that no significant disturbance produced by the resonator was observed for this series of tests.

E. PVC APPARATUS

The flow was not choked for this series of tests, and the microphone was placed back into the motor. The aperture diameter remained at 0.25 inches,

TABLE IV.vi FREQUENCY PREDICTED BY PANTON

c ft/s	d_o in	H in	d in	t in	l′ in	λ in	$(f_o)_t$ Hz
1,117	0.25	4.245	1.06	0.031	0.212	2.473	451.9
1,117	0.25	5.245	1.06	0.031	0.212	2.834	394.2

although its thickness was changed to 0.06 inches. The upstream pipe and T-fitting were changed from stainless steel to PVC piping of the same diameter. This represented one of many attempts to decrease the system noise. There was an irregular wavy pattern on the inside surface of the PVC pipe but it was not enough to have a noticeable effect on the flow. These waves were very smooth and of very low amplitude, not more than up to 0.06 inches. The aperture was changed from the Teflon-copper plug to bondo. The bondo, although permanently set in the hole, could be adjusted with a drill. Tests #21 - 25 were completed using this configuration. The observed amplitude of these tests were nearly uniform so no data was taken. Changing from stainless steel to PVC neither canceled nor reduced the noise observed.

F. MEASUREMENTS FOR UNCHOKED FLOW

The sound spectra were plotted using the HP X-Y plotter for the remaining tests of this experiment. (Refer to Table IV.iii.) RECORD's #1 - 7 were for unchoked flow. The pressure gauge for the aft combustion chamber was changed from the 0 - 300 psi gauge to the 0 - 5000 psf gauge in order to obtain a more accurate reading. Only one pressure was measured so the velocity could not be determined. However, it was assumed that the Reynolds number was greater than the critical value so that the flow was turbulent. Only noise was observed in the spectra, which did not change with resonator cavity length.

G. MEASUREMENTS WITHOUT THE MOTOR INSTALLED

The motor was removed, and not replaced for the remaining tests. The remainder of the tests concentrated on trying to find a resonator configuration that would produce noticeable effects and it was thought that the engine would only complicate that search. The flow was again not choked. The diameter of the aperture was enlarged to 0.31 inches, while the thickness was kept at 0.06 inches. The diameter of the cavity was 1.06 inches. The sound spectra were observed for two different cavity lengths, at this new aperture diameter. No change in the spectra were observed and no X-Y plots were made. The aperture was then enlarged to 0.38 inches in diameter and the amplitude of the spectra were observed to change with change in cavity length at selected frequencies. It is noted here that further diameter enlargements were made but the most noticeable change in response was at this (0.38 inches) aperture diameter. Pitot and static pressure tubes were installed to determine the velocity passing over the resonator orifice. Table IV.vii shows these pressure measurements, P_t being the total pressure and P_s the static. The total pressure read from the gauge (first column) was corrected for the reading of the gauge (+0.15 H_2O) when no pressure was applied to the gauge. This error was assumed to apply to all readings. These measured velocities are comparable to those of Panton (Panton, 1990).

H. CHOKED FLOW MEASUREMENTS

This next set of tests were performed with the nozzle reinstalled choking the flow. Choked flow is most important in this experiment since the flow

TABLE IV.vii CALCULATED VELOCITIES FOR UNCHOKED FLOW

P_t In. H_2O	P_t psfg	P_s psfg	ΔP psf	U ft/s	U mph
40	206.94	166	40.9	178.88	121.96
60	310.80	255	55.8	208.84	142.39
80	414.66	347	67.7	229.96	156.79
100	518.52	438	80.5	250.87	171.04

NOTE: P_t & P_s were measured separately

upstream of the hybrid rocket motor exit nozzle will only be choked for optimum operation. The static and stagnation pressures were measured to compute the velocity. However the two gauges used to determine the velocities had such different scales that it was difficult to accurately determine the pressure difference for low velocities. For these velocities, the gauges gave negative pressure differential values which is meaningless. The velocity could only be estimated using compressible flow theory (refer to section C) and the measured static pressure. No discernible SPL peaks were noted for the choked flows, RECORD's #10 - 18.

I. MICROPHONE PLACED INSIDE CAVITY

The microphone was installed in the bottom of the cavity of the Helmholtz resonator, through the endcap. This prevented changing the cavity lengths by changing the number of spacers within the cavity. Instead, the length of the cavity was changed by using bodies of different lengths, as discussed in Chapter III. The lengths of the cavities were 3.25, 4.63, 7.25 and

9.25 inches. Predicted resonant frequencies for each of these cavity lengths are listed in Table IV.viii. Since only noise was observed, only one spectra was produced.

Although the sound spectra were measured inside the resonator, no differences were observed between different cavity lengths of 3.25 and 4.63 inches. The aperture diameter was increased to 0.31 inches and still no spectra peaks that varied with the resonator length were observed. The aperture was increased to 0.38 inches in diameter and again there was no change in the spectra for the two lengths.

J. APERTURE THICKNESS INCREASED GREATLY

A summary of the data collected from RECORD's #21 - 73 (refer to Table IV.iii) was completed. Tables IV.ix - IV.xiv, and Figures 4.2 - 4.7 which compile the data gathered from the X-Y plots for the choked flows; each figure has an accompanying table, as follows.

TABLE IV.viii PREDICTED RESONATOR FREQUENCIES USING EQUATION (2.14)

c ft/s	d_o in	H in	d in	t in	l′ in	λ in	$(fo)_t$ Hz
1,117	0.25	3.250	1.0625	0.25	0.431	2.812	397.4
1,117	0.25	4.625	1.0625	0.25	0.431	3.440	324.8
1,117	0.25	7.250	1.0625	0.25	0.431	4.504	248.1
1,117	0.25	9.250	1.0625	0.25	0.431	5.251	212.8

do in	INSIDE TABLE	INSIDE FIGURE	OUTSIDE TABLE	OUTSIDE FIGURE
0.38	IV.ix	4.2	IV.x	4.3
0.44	IV.xi	4.4	IV.xii	4.5
0.50	IV.xiii	4.6	IV.xiv	4.7

Each figure shows a series of spectral plots, and a corresponding table to each figure, containing the numerical data, each labeled. In each table there are four columns, one for each cavity length. Even for those where only two lengths were used, four are still listed for easy comparison. Pairs of tables account for frequency measurements taken outside and inside the cavities, respectively, one pair for each aperture diameter. The tables include noted frequency peaks, relative to the overall plot, and their respective SPL's. As usual, all choked flows are assumed to be turbulent.

The thickness of the aperture was changed since changing the orifice diameter was not producing measurable results. The thickness was increased rather drastically to 1.33 inches. This made the resonator appear more as a long-necked bottle. With the microphone in the cavity, a resonant frequency peak of 192 Hz was measured for the 7.25-inch length cavity. For the 9.25-inch length cavity that peak moved down to 172 Hz. In order to compare these to theoretical predictions, calculations were performed using equations, (2.14) and (2.15), to determine the expected resonant frequency, along with equation (2.10) and (2.13) for predicting the higher order modes. The predictions of the four cavity lengths using these equations for four different aperture diameters are given in Table IV.xv.

Fourteen measured spectra for four cavity lengths are shown in Figure

TABLE IV.ix CORRESPONDING PLOT IN FIGURE 4.2, CHOKED FLOW, INSIDE CAVITY

H = 3.25"

fo Hz	SCALE dB	SPL dB
208	-19.4	108.6
256	-5.9	122.1
348	-12.9	115.1
372	-14.1	113.9
396	-15.4	112.6
420	-16.4	111.6
512	-14.6	113.4
620	-15.7	112.3

fo Hz	SCALE dB	SPL dB
256	-5.5	122.5
348	-11.8	116.2
372	-13.1	114.9
396	-14.1	113.9
420	-14.9	113.1
512	-14.7	113.3
632	-14.3	113.7

H = 4.63"

fo Hz	SCALE dB	SPL dB
236	-12.4	115.6
256	-5.2	122.8
292	-11.3	116.7
340	-12.4	115.6
512	-15.3	112.7

fo Hz	SCALE dB	SPL dB
240	-11.3	116.7
256	-4	124.0
292	-8.9	119.1
336	-12.2	115.8
368	-16	112.0
516	-12.4	115.6
628	-16.2	111.8

H = 7.25"

fo Hz	SCALE dB	SPL dB
192	-10.1	117.9
260	-9.6	118.4
292	-12.5	115.5
828	-13.1	114.9

fo Hz	SCALE dB	SPL dB
200	-5.1	122.9
260	-3.6	124.4
292	-5.8	122.2
336	-8.4	119.6
396	-8.7	119.3
429	-10.8	117.2

fo Hz	SCALE dB	SPL dB
192	-10.8	117.2
256	-12.7	115.3
380	-14.9	113.1
828	-20.1	107.9
908	-19.4	108.6

fo Hz	SCALE dB	SPL dB
204	-9.4	118.6
256	-11.2	116.8
336	-17.3	110.7
400	-15.1	112.9

H = 9.25"

fo Hz	SCALE dB	SPL dB
164	-11.2	116.8
256	-8.2	119.8
316	-11.4	116.6
400	-14.2	113.8

fo Hz	SCALE dB	SPL dB
172	-12.9	115.1
252	-14.7	113.3

fo Hz	SCALE dB	SPL dB
108	-17.8	110.2
172	-12.6	115.4
256	-16.6	111.4
332	-16.7	111.3
512	-21.4	106.6
752	-19.7	108.3

fo Hz	SCALE dB	SPL dB
104	-17.9	110.1
168	-12.4	115.6
256	-17.1	110.9
280	-18.3	109.7
332	-16.9	111.1
512	-21.3	106.7
748	-19.8	108.2

fo Hz	SCALE dB	SPL dB
172	-13.3	114.7
256	-17.3	110.7
332	-16.4	111.6
508	-21.6	106.4
784	-18	110.0

fo Hz	SCALE dB	SPL dB
172	-16.4	111.6
256	-17.2	110.8
332	-20.8	107.2
372	-21.9	106.1
516	-25.3	102.7

CONSTANTS

do = 0.38"
d = 1.06"
t = 1.31"

TABLE DEFINITIONS

outside - microphone outside of resonator
inside - microphone inside of resonator cavity
scale - data read directly from Spectrum Analyzer

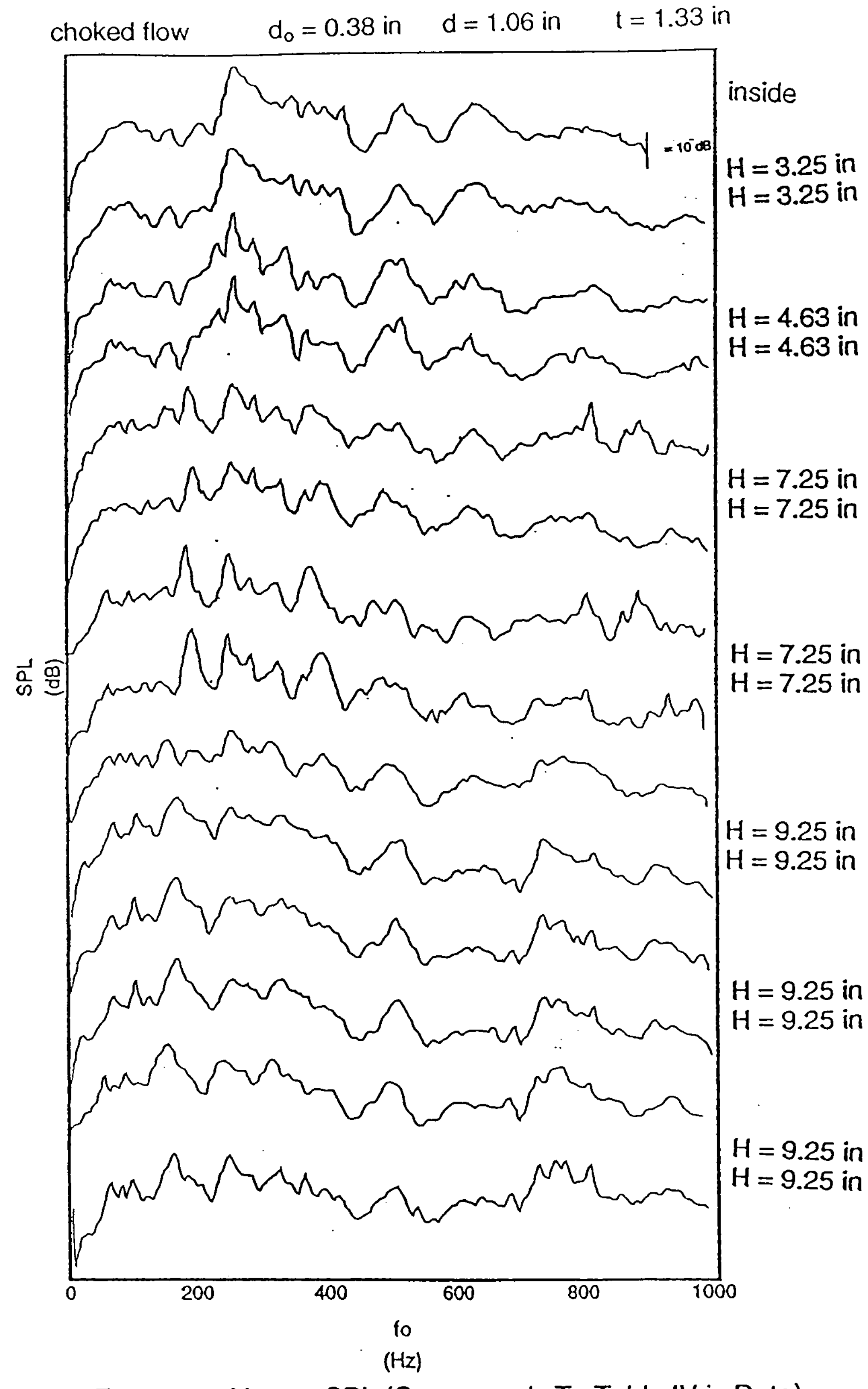

Figure 4.2 Frequency Versus SPL (Corresponds To Table IV.ix Data)

TABLE IV.x CORRESPONDING PLOT IN FIGURE 4.3, CHOKED FLOW, OUTSIDE CAVITY

H = 3.25"

fo Hz	SCALE dB	SPL dB

H = 4.63"

fo Hz	SCALE dB	SPL dB

H = 7.25"

fo Hz	SCALE dB	SPL dB
256	-19.4	108.6
288	-18.9	109.1
332	-14.5	113.5
368	-17.7	110.3
420	-16.6	111.4
508	-19.8	108.2
824	-13.3	114.7

H = 9.25"

fo Hz	SCALE dB	SPL dB
68	-21.4	106.6
108	-20.8	107.2
260	-20	108.0
288	-21.3	106.7
332	-16.4	111.6
368	-22.1	105.9
396	-22.2	105.8
420	-21.4	106.6
512	-26.3	101.7
828	-20.5	107.5

68	-21.7	106.3
256	-18.7	109.3
292	-18.7	109.3
332	-14.1	113.9
368	-17.1	110.9
420	-18.7	109.3
512	-19.4	108.6
828	-16.4	111.6

256	-14.7	113.3
292	-15.2	112.8
332	-10.9	117.1
368	-15.4	112.6
396	-15.9	112.1
420	-15.3	112.7
472	-19.2	108.8
504	-19	109.0
828	-14	114.0

CONSTANTS

do = 0.38"
d = 1.06"
t = 1.31"

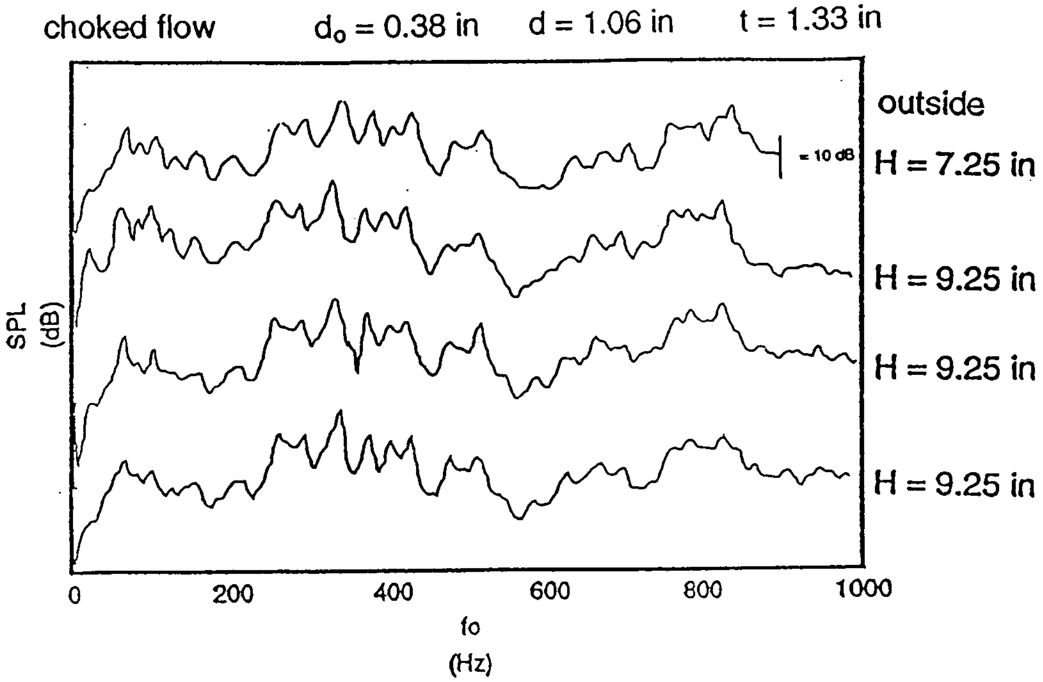

Figure 4.3 Frequency Versus SPL (Corresponds To Table IV.x Data)

TABLE IV.xi CORRESPONDING PLOT IN FIGURE 4.4, CHOKED FLOW, INSIDE CAVITY

H = 3.25"

fo Hz	SCALE dB	SPL dB
204	-13.1	114.9
256	-2.8	125.2
324	-5.8	122.2
396	-3.1	124.9
656	-7.6	120.4

fo Hz	SCALE dB	SPL dB
268	-10.4	117.6
396	-13.9	114.1
624	-20.7	107.3

H = 4.63"

fo Hz	SCALE dB	SPL dB
212	-13.3	114.7
256	0.1	128.1
292	-5.5	122.5
516	-7.5	120.5

fo Hz	SCALE dB	SPL dB
260	3.4	131.4
292	-2.1	125.9
516	-4.3	123.7
632	-6.6	121.4

H = 7.25

fo Hz	SCALE dB	SPL dB
160	-19.9	108.1
216	-9.6	118.4
256	-12.5	115.5
336	-15.6	112.4

fo Hz	SCALE dB	SPL dB
156	-19.5	108.5
216	-7.3	120.7
256	-9.6	118.4
336	-13.8	114.2
432	-17.3	110.7
472	-18	110.0
508	-17.2	110.8

H = 9.25"

fo Hz	SCALE dB	SPL dB
168	-15.3	112.7
188	-11.3	116.7
256	-14.9	113.1
376	-14.2	113.8
516	-19.1	108.9
768	-17.7	110.3
256	-17.2	110.8

fo Hz	SCALE dB	SPL dB
108	-18.4	109.6
188	-11.3	116.7
256	-13.5	114.5
376	-14.8	113.2
516	-20.1	107.9
736	-18.4	109.6
828	-19.3	108.7

CONSTANTS

do = 0.44"
d = 1.06"
t = 1.31"

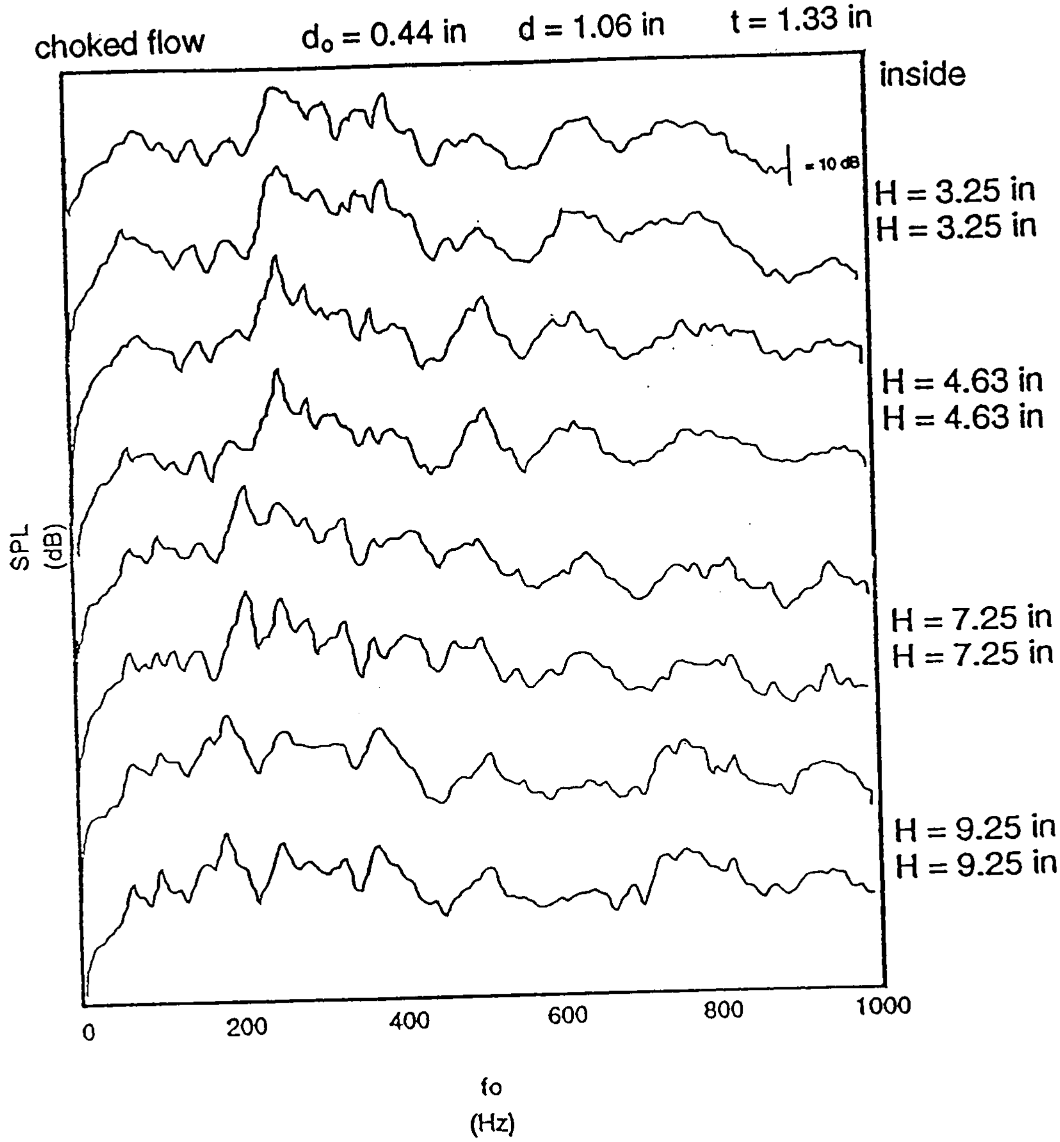

Figure 4.4 Frequency Versus SPL (Corresponds To Table IV.xi Data)

TABLE IV.xii CORRESPONDING PLOT IN FIGURE 4.5, CHOKED FLOW, OUTSIDE CAVITY

H = 3.25"

fo Hz	SCALE dB	SPL dB

H = 4.63"

fo Hz	SCALE dB	SPL dB
256	-11.6	116.4
372	-13.3	114.7
828	-10.1	117.9

fo Hz	SCALE dB	SPL dB
256	-9.2	118.8
372	-10.2	117.8
420	-10.9	117.1
516	-14.3	113.7
828	-7.2	120.8

H = 7.25"

fo Hz	SCALE dB	SPL dB
212	-22.4	105.6
336	-18.1	109.9
372	-18.7	109.3
420	-20.1	107.9
512	-20.8	107.2
752	-19.3	108.7
828	-16.7	111.3

fo Hz	SCALE dB	SPL dB
292	-19.7	108.3
340	-15.5	112.5
372	-16.8	111.2
420	-19.1	108.9
512	-21.2	106.8
828	-14.1	113.9

H = 9.25"

fo Hz	SCALE dB	SPL dB
264	-20.1	107.9
332	-14.6	113.4
372	-19.5	108.5
420	-19.4	108.6
512	-20.4	107.6

CONSTANTS

do = 0.44"
d = 1.06"
t = 1.31"

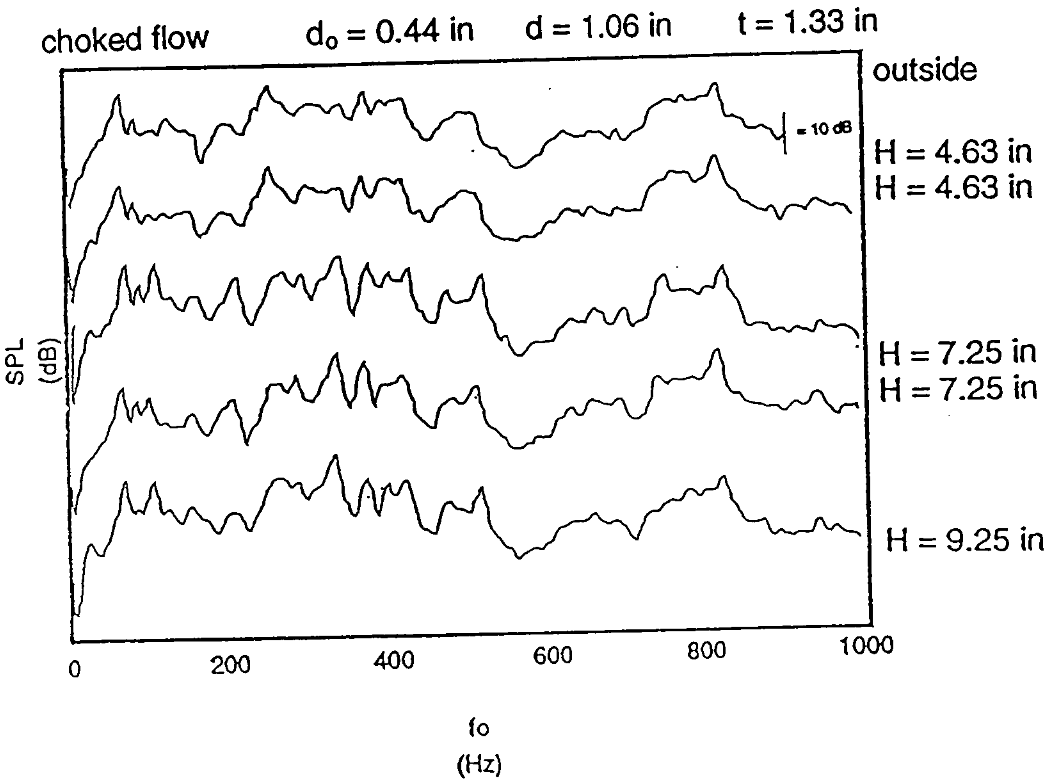

Figure 4.5 Frequency Versus SPL (Corresponds To Table IV.xii Data)

TABLE IV.xiii CORRESPONDING PLOT IN FIGURE 4.6, CHOKED FLOW, INSIDE CAVITY

H = 3.25"

fo Hz	SCALE dB	SPL dB

H = 4.63"

fo Hz	SCALE dB	SPL dB

H = 7.25

fo Hz	SCALE dB	SPL dB
232	-12.1	115.9
256	-7.1	120.9
292	-11.8	116.2
372	-15.6	112.4

fo Hz	SCALE dB	SPL dB
232	-19.5	108.5
256	-7.3	120.7
292	-9.6	118.4
340	-13.8	114.2
372	-17.3	110.7
510	-18	110.0

H = 9.25"

fo Hz	SCALE dB	SPL dB
164	-17.2	110.8
200	-8.2	119.8
272	-13.2	114.8
308	-15.3	112.7
400	-13.1	114.9

fo Hz	SCALE dB	SPL dB
204	-9.2	118.8
256	-13.4	114.6
400	-13.1	114.9

CONSTANTS

do = 0.5"
d = 1.06"
t = 1.31"

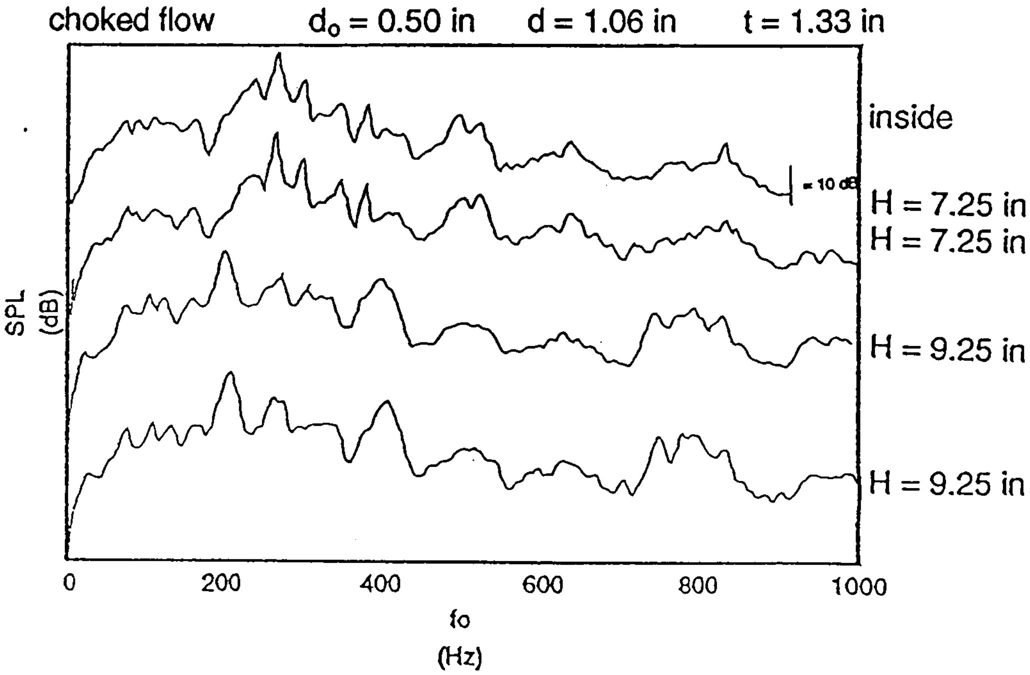

Figure 4.6 Frequency Versus SPL (Corresponds To Table IV.xiii Data)

TABLE IV.xiv CORRESPONDING PLOT IN FIGURE 4.7, CHOKED FLOW, OUTSIDE CAVITY

H = 3.25"

fo Hz	SCALE dB	SPL dB

H = 4.63"

fo Hz	SCALE dB	SPL dB

H = 7.25"

fo Hz	SCALE dB	SPL dB
340	-18.3	109.7
372	-17.4	110.6
516	-21.9	106.1
756	-18.5	109.5
832	-14.6	113.4

296	-19.8	108.2
340	-15.8	112.2
372	-13.8	114.2
412	-19	109.0
516	-19.5	108.5
828	-12.1	115.9

H = 9.25"

fo Hz	SCALE dB	SPL dB
108	-17.8	110.2
336	-15.8	112.2
372	-14.8	113.2

72	-21.4	106.6
108	-22.5	105.5
256	-21.2	106.8
336	-16.2	111.8
372	-19.2	108.8
420	-20.4	107.6
516	-21.9	106.1
832	-17.9	110.1

CONSTANTS

do = 0.5"
d = 1.06"
t = 1.31"

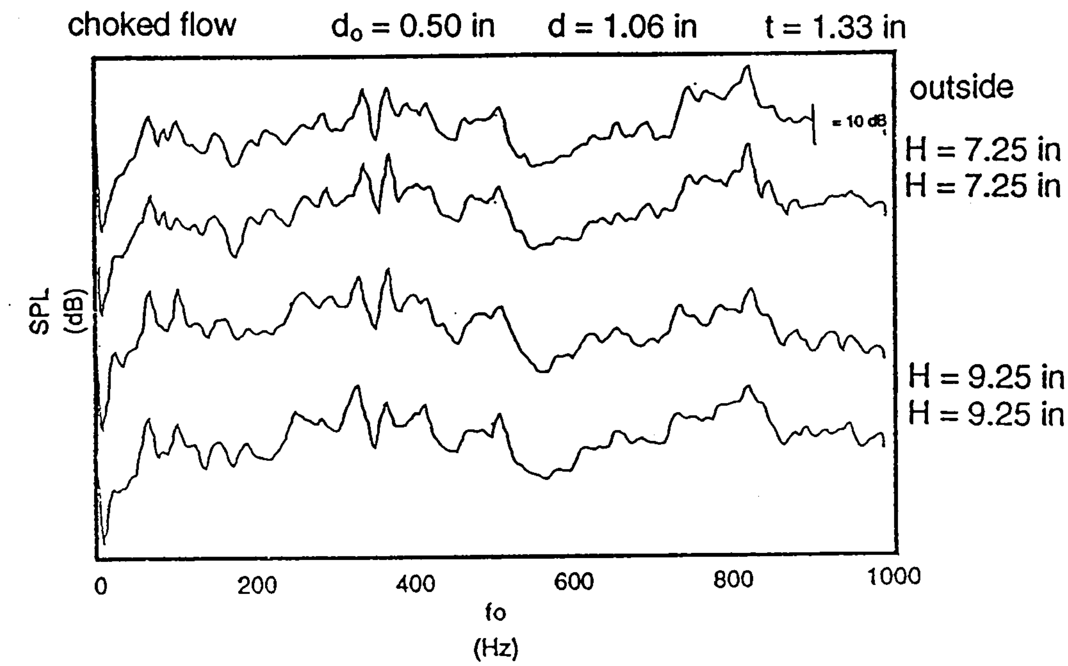

Figure 4.7 Frequency Versus SPL (Corresponds To Table IV.xiv Data)

TABLE IV.xv PANTON'S THEORETICAL f_o PREDICTIONS

	H = 9.25"	H = 7.25"	H = 4.63"	H = 3.25"
d_o = 0.50"				
n = 0	215.60	252.50	332.50	408.00
1	508.30	671.10	1115.20	1652.30
2	1232.20	1594.70		
3	1956.10			
d_o = 0.44"				
n = 0	197.30	230.00	299.40	365.20
1	526.60	694.10	1148.40	1695.10
2	659.20	1617.60		
3	1974.40			
d_o = 0.38"				
n = 0	176.60	204.20	263.90	320.20
1	547.30	719.40	1183.90	1740.10
2	1271.20	1643.00	1395.70	
3	1397.90			
d_o =0.31"				
n = 0	153.40	176.30	225.90	272.90
1	570.40	747.27	1221.90	1787.50
2	1294.30	1670.90		
3	2018.20			

d = 1.06"
t = 1.31"
n - overtone

4.2. The aperture diameter was 0.38 inches. Those for the 9.25-inch cavity length were measured within the cavity. The measured resonant frequency for each was 172, 172, 168 and 172 Hz, which is a three percent or less error. The spectra corresponding to the 7.25-inch cavity had resonant frequencies of 204, 192, 200 and 192 Hz, respectively, which was up to six percent below predictions, the next pair of spectra taken with the 4.63-inch cavity appeared to enhance the 256 Hz peak that had been observed in the background spectra. The predicted resonant frequency for this cavity length is 264 Hz. Finally, the last pair of spectra, where H = 3.25 inches, has a noticeably peak at about 350 Hz, compared to the other spectra. Its theoretical resonant frequency is 320 Hz, but the peak is not sharp enough to state whether it is due to background noise, or the resonator. Following these measurements, many more spectra were taken mainly using the 9.25 and 7.25-inch length cavities because no discernible frequency peaks were observed inside or outside the two shorter cavities. This is probably due to the fact that the background SPL was higher for the shorter cavity lengths, and more easily covered up the sound created by the resonator than for the deeper resonators.

Although the resonant excitations were found for the deeper cavities, the peaks were not high. There is little chance the Helmholtz resonator will have any effect downstream, especially in the precombustion chamber. Outside the cavity, the peaks were greatly attenuated. Measurements made outside are shown in Figure 4.3 and they should be compared to those measured inside in Figure 4.2. The two sets of measurements were made under the same conditions. No height of excitation at the resonator frequency can be observed in Figure 4.3 (Also refer to Table IV.x.)

It appeared that although there was a response from the resonator for choked flow from measurements made inside the cavity, the resonant peaks were still only slightly greater than the noise peaks, although there was a noticeable response for apertures equal to or larger than 0.38 inches, and for 7.25- and 9.25-inch cavity lengths. For this reason most of the data was collected for these lengths. In general, though, the 256 and 800 Hz peaks overwhelmed anything else.

K. UNCHOKED FLOWS AT LOWERED VELOCITIES

In this final section, spectra were measured for unchoked flow without the motor. These velocities, 56, 96, and 143 ft/s, were measured with the static and pitot probes. These are within the range of those used in Panton, 1990. The difference between static and total pressure was measured directly, using the psig gauge. Table IV.xv lists the noted frequency peaks, and the corresponding SPL values. (Refer to Figures 4.8 - 4.10 for the spectra of unchoked flow.) No discernible peaks were observed in the spectra.

For the final test the cavity was removed and the aperture plugged so H=d=0 essentially. No distinct frequencies noted (see Figure 4.11 for measurements at each velocity). In this case the frequency span in the figure is 5 kHz. Higher spans were examined to make sure that high frequency resonances were not occurring, but none were discovered.

TABLE IV.xvi CORRESPONDING PLOTS IN FIGURES 4.8 - 4.10, UNCHOKED FLOW

U = 56 ft/s

fo Hz	SCALE dB	SPL dB

H = 9.25"
OUTSIDE*

160	-33.0	95.0
260	-31.3	96.7
810	-31.5	96.5
950	-31.8	96.2

H = 7.25"
OUTSIDE

170	-32.3	95.7
290	-36.5	91.5
780	-27.1	100.9
930	-32.4	95.6
1240	-35.9	92.1

H = 9.25"
INSIDE

200	-24.1	103.9
260	-24.1	103.9
790	-22.5	105.5
960	-31.8	96.2
1580	-42.2	85.8
1990	-46.7	81.3
2190	-47.8	80.2

H = 7.25"
INSIDE

260	-21.2	106.8
810	-25.5	102.5
1650	-32.9	95.1
1990	-26.3	101.7

U = 96 ft/s

fo Hz	SCALE dB	SPL dB

H = 9.25"
OUTSIDE

160	-29.9	98.1
260	-27.1	100.9
800	-29.9	98.1
950	-31.9	96.1
1240	-31.5	96.5
1580	-30.0	98.0
1680	-31.5	96.5
2010	-32.7	95.3

H = 7.25"
OUTSIDE

400	-28.8	99.2
780	-25.9	102.1
1240	-30.9	97.1
1580	-28.7	99.3

H = 9.25"
INSIDE

260	-19.3	108.7
790	-19.5	108.5
970	-26.4	101.6
1580	-33.4	94.6
1980	-32.6	95.4
2180	-31.4	96.6

H = 7.25"
INSIDE

260	-19.0	109.0
950	-31.8	96.2
1240	-37.1	90.9
2000	-29.4	98.6

U = 143 ft/s

fo Hz	SCALE dB	SPL dB

H = 9.25"
OUTSIDE

800	-22.8	105.2
960	-29.5	98.5
1230	-29.7	98.3
1580	-28.1	99.9
1660	-21.4	106.6

H = 7.25"
OUTSIDE

770	-23.0	105.0
1230	-30.9	97.1
1580	-28.1	99.9
1650	-21.5	106.5

H = 9.25"
INSIDE

260	-23.1	104.9
800	-15.8	112.2
990	-26.1	101.9
1560	-28.9	99.1
1990	-34.5	93.5
2170	-31.3	96.7

H = 7.25"
INSIDE

260	-21.2	106.8
810	-25.5	102.5
1650	-32.9	95.1
1990	-26.3	101.7

CONSTANTS

d = 1.06"
do = 0.50"
t = 1.31"

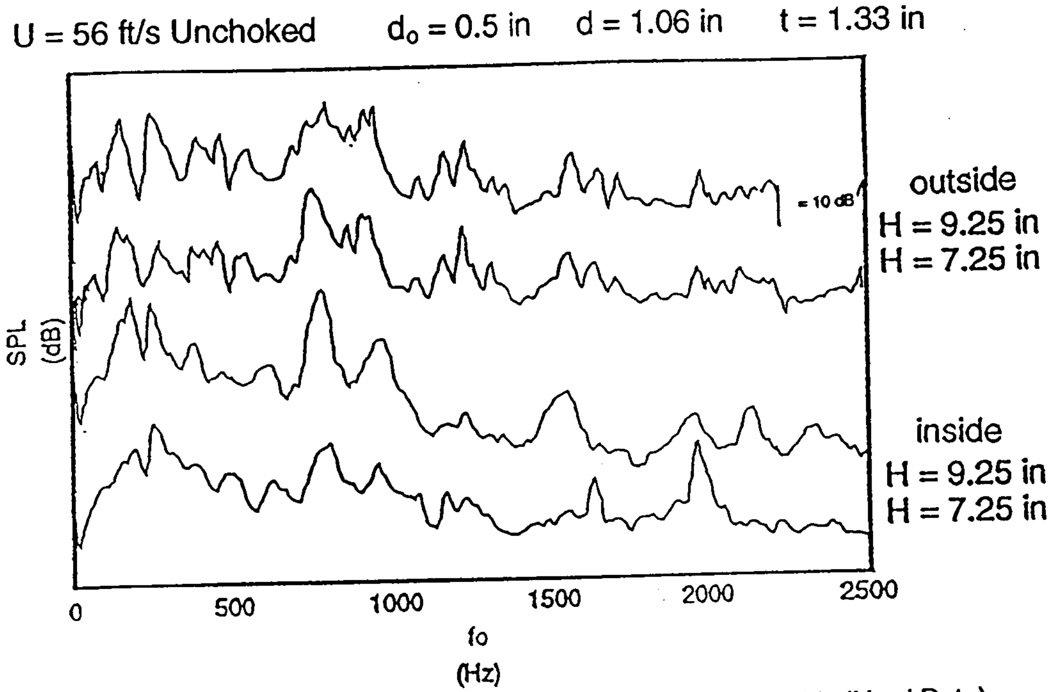

Figure 4.8 Frequency Versus SPL, U = 56 ft/s (Corresponds To Table IV.xvi Data)

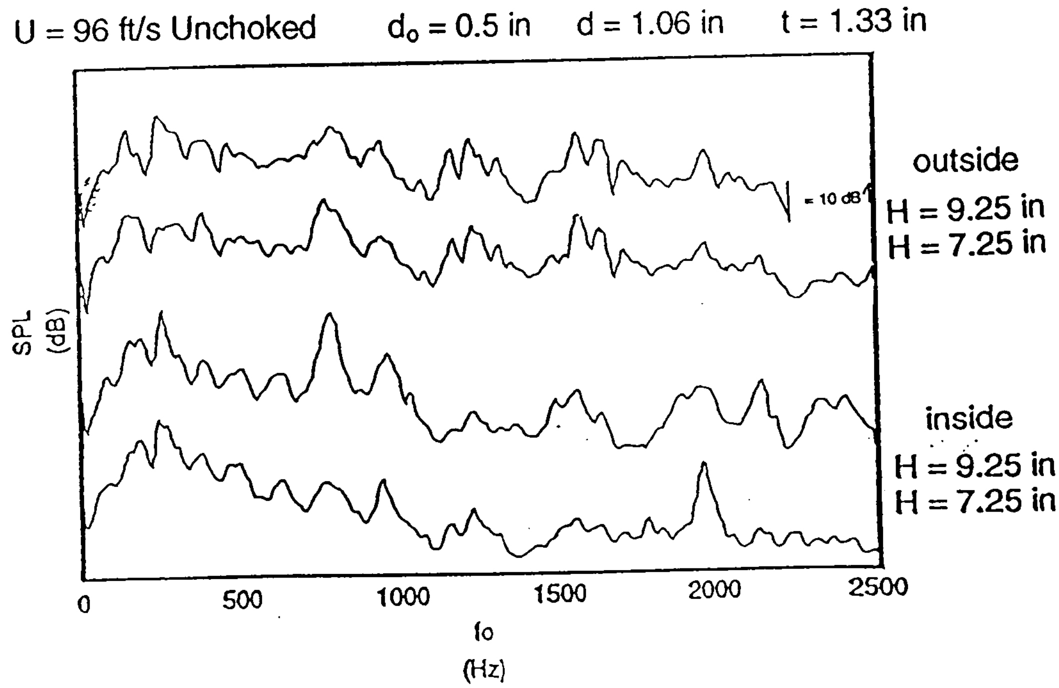

Figure 4.9 Frequency Versus SPL, U = 96 ft/s (Corresponds To Table IV.xvi Data)

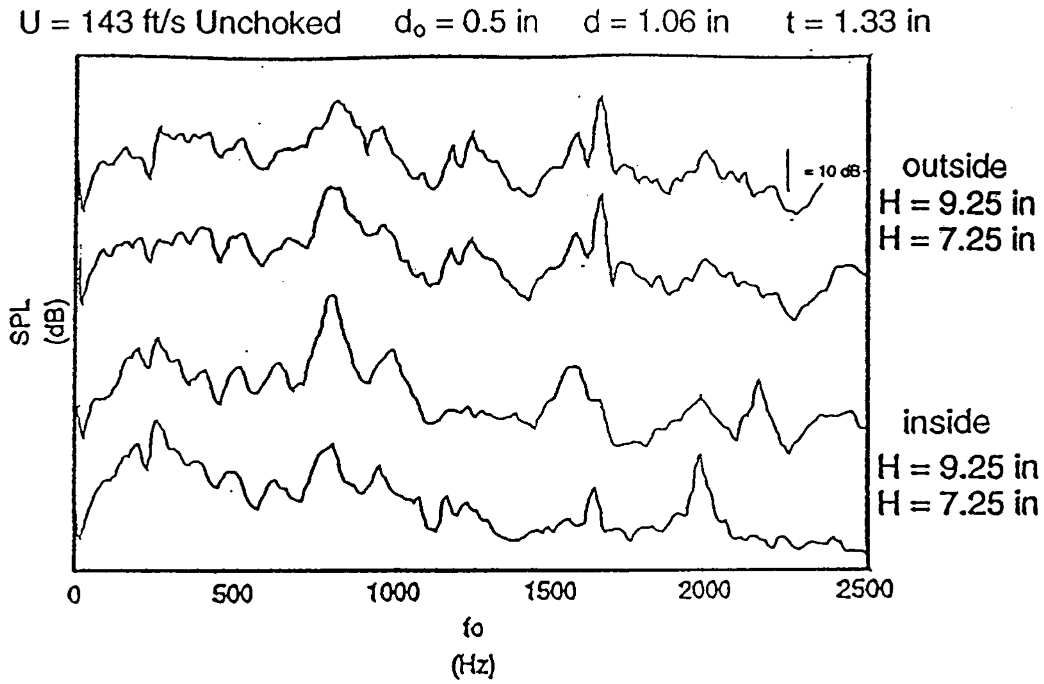

Figure 4.10 Frequency Versus SPL, U = 143 ft/s (Corresponds To Table IV.xvi Data)

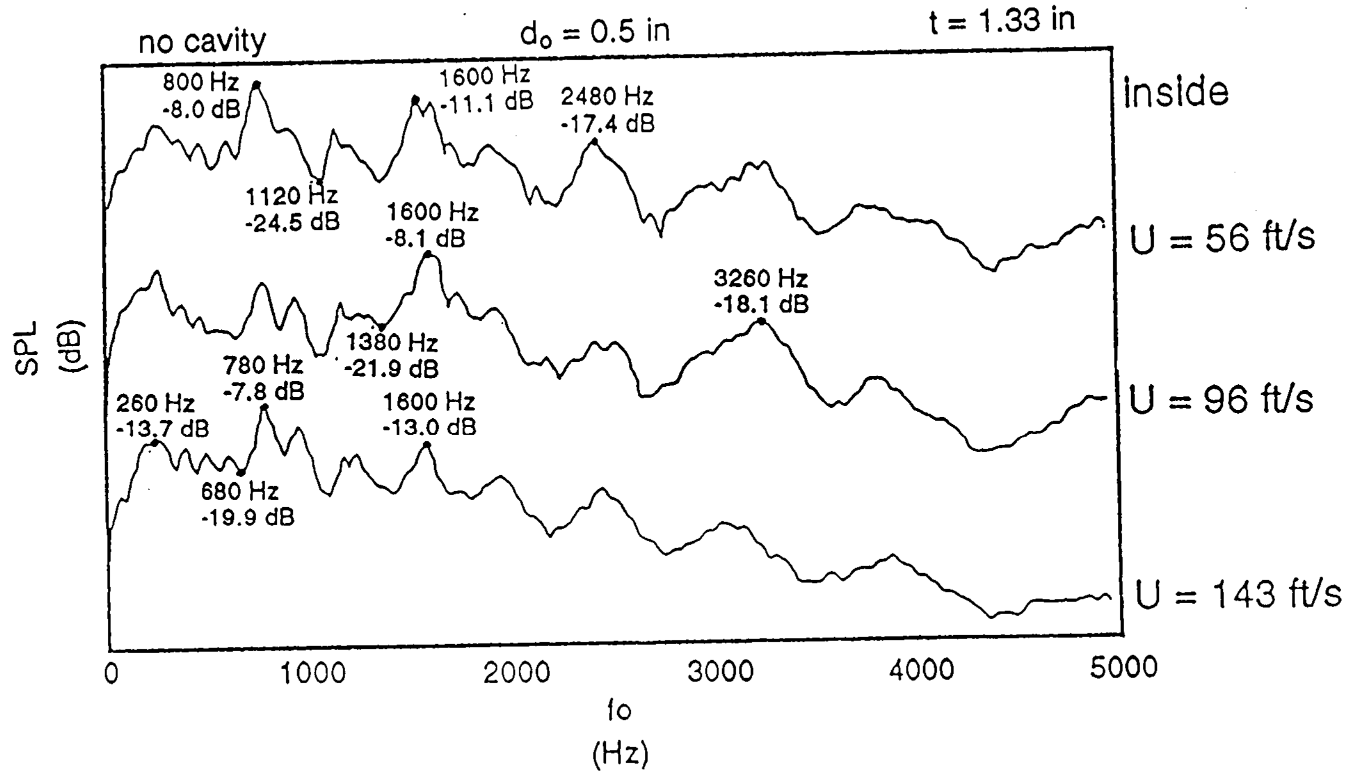

Figure 4.11 Frequency Versus SPL: Cavity Blocked Off Completely

CHAPTER V

CONCLUSIONS

A. SUMMARY

There were two sets of meaningful data in this experiment. Significant SPL peaks were detected at 1250 Hz in the hybrid rocket motor precombustion chamber for choked flow, and measured resonance occurred inside the Helmholtz resonator for a geometry of t = 0.38 inches, d = 1.06 inches, d_o = 1.3 inches, and 3.25 < H < 9.25 inches. Otherwise, no meaningful spectra were observed. No resonator excitations were of great enough amplitude to be observed in the hybrid motor precombustion chamber. The 1250 Hz peak was caused by the Helmholtz resonator orifice plate protruding into the pipe leading to the hybrid motor and not the motor itself. Therefore, it is concluded that the Helmholtz resonator is not a suitable means for exciting the hybrid motor flow.

B. SIGNIFICANT DATA

The 1250 Hz peak in the SPL spectra was observed in the precombustion chamber of the hybrid motor when the orifice plate of the Helmholtz resonator protruded approximately 0.06 inches into the flow stream. It was the only disturbance observed within the hybrid motor. This disturbance is caused by the time-dependent shear layer separation on the downstream portion of the protuberance. Since it is a passive disturbance source future investigations should further explore this means of stimulating the hybrid motor precombustion chamber flow. The relationship between the protuberance height, pipe velocity, and disturbance frequency and amplitude should be determined.

Measured resonance of the Helmholtz resonator was only observed for one geometry with the microphone placed inside the resonator cavity; no disturbance was observed outside the resonator, in the oxidizer line. The absence of resonator response using other geometries was thought to be due to the low amplitude of the resonator response and the large amplitude of the background noise of the system. Equation (2.17) states that as $\mathbf{x} \to \infty$ $P' \to 0$. It should be noted, however, that this equation is for a uniform flow over the piston while the present experiment included a boundary layer. It can be expected that this boundary layer would further attenuate the far field pressure fluctuations.

Equation (2.17) implies that as $|\mathbf{x}| \to D_p$ the cavity pressure effect on the oxidizer line pressure decreases. This reduction probably is the reason why the microphone did not measure a peak in the SPL for the same geometry that it did inside the resonator. Also, equation (2.17) predicted a higher SPL than obtained in the frequency spectra. For example, for H = 7.25 inches plotted in Figure 4.2 the predicted SPL is 158 dB measured at $|\mathbf{x}| = D_p$. Figure 4.2 frequency spectra displays a much lower SPL of approximately 110 dB. Attentuation through the turbulent boundary layer is probably the cause.

C. ADDITIONAL CONSIDERATIONS AND CONCLUSIONS

Observed changes in spectra followed no pattern based on resonator geometrical adjustments. This was probably because the test set-up used in this particular experiment differed so much from that used in Panton (17 & 18).

A horn was used to excite the resonators in one experiment, and a large diameter wind tunnel in the other, and the system noise was low in both cases.

The measuring devises in this experiment, including the Spectrum Analyzer, condenser microphone and X-Y plotter, were tested for accuracy. There are two types of B & K quarter-inch diameter condenser microphones; type 4136 was used in this experiment. Refer to Appendix 2 for the dynamic range, and graphs of the directional and distortional characteristics of this microphone. This microphone was able to measure the frequency response in this experiment quite accurately (B & K, 1982). The spectrum analyzer was tested and found to be in excellent working order with minimal error that would not effect the data collected in this experiment. Inaccuracies due to a lack of plotting paper had negligible effect on the overall results.

The stainless steel oxidizer pipe and T-fitting were replaced with PVC in order to reduce unwanted noise. The connection between the 2 to 1.5 inch reducer and the PVC line was smoothed out with bondo. This change did not effect the noise of the system.

Upstream of the apparatus the two-inch diameter air supply pipe contained four ninety degree turns in it, the closest turn being 6.6 feet upstream of the resonator. These turns were a permanent part of the upstream piping and could not be removed. Flow straighteners might have settled the flow somewhat, but were not employed for this configuration. None of the noise frequencies seemed to correspond to organ pipe modes of the upstream lengths of pipe.

The air came from a very large, high pressure air tank, pressurized up to a maximum of 600 psig. The flow entered the piping in the laboratory and passed through two ball valves, which were 22.75 feet apart. Between these valves are the four previously mentioned ninety degree turns. These valves cannot be guaranteed as completely open, but a very small protrusion would probably produce a higher discernible frequency peak, like the Teflon-copper plug , than those observed.

Another possible protrusion considered was the static pressure probe in the oxidizer line. It was made from a 0.06-inch diameter tube. Also, the possibility of the microphone protruding into the flow was immediately ruled out since the disturbance was known when it did protrude. In that case the SPL had a discernible peak at 330 Hz. The last noise source considered was the blank flange with the exit nozzle hole. This flange contained a one-inch exit hole at the end of the 1.5-inch line, producing a reduction of 0.5 inches in diameter. The flow will hit the sharp straight edges of the exit hole and generate a disturbance in the shear layer.

Although protrusions are possible causes of the noise that was observed, they were probably not the likely source since none of the background noise varied with the flow velocity, a requirement for protrusions, as the definition of the Strouhal number predicts.

Another possible source of the unwanted noise considered that was independent of velocity was the pipe sections each acting like organ pipes, developing a resonant frequency, dependent only on their length. In this apparatus, each section of tube was considered. The resonant frequency for each pipe section was calculated along with the respective first and second overtones. None of these gave the frequency peaks repeatedly observed, i.e., 260 or 800 Hz.

D. FINAL CONCLUSION

The Helmholtz resonator did not prove to be a useful source for introducing disturbances into a hybrid rocket motor. However, the spectra due to the Teflon-copper plug protrusion was the most important discovery in this experiment, because it was the only observed tone that traveled downstream in choked flow into the combustion section. According to the Strouhal number this type of protrusion will vary the resonant frequency with its own height variation. If true this would be a simpler system to employ than the Helmholtz resonator. The resonator is not needed, since the resonant frequency can be varied by varying the height of the protrusion. Therefore, a desired frequency can be set.

CHAPTER VI

RECOMMENDATIONS FOR FUTURE WORK

This experiment disproves the idea that employing a passive way of disturbing the flow using a Helmholtz resonator will have an effect on the precombustion chamber turbulent mixing for the configuration described in Chapter III since it did not produce disturbances with amplitudes above the system noise in the oxidizer line, and had no effect on the frequency spectrum in the precombustion chamber. Unexpectedly though, another useful passive method was found. An unwanted protrusion inside the oxidizer line, produced by the Teflon-copper plug, produced a resonant frequency of 1250 Hz that was observed in the hybrid rocket motor precombustion chamber, while the Helmholtz resonator only produced measured resonant frequencies inside its cavity for one specific geometry. If the frequency tone in the combustor does increase the turbulent mixing, hence the fuel regression rate, then the protrusion in the oxidizer line is an important discovery.

In regards to actual tests, it is recommended that several cold flow tests be performed, varying the protrusion height for each. If a measured change in the resonant frequency occurs due to a change in protrusion height (Strouhal number), then the motor should be run with gaseous or liquid oxygen, and solid plexiglass. No further use of the Helmholtz resonator is recommended.

LIST OF REFERENCES

LIST OF REFERENCES

1. Alster, M., "Improved Calculation of Resonant Frequencies of Helmholtz Resonators," Journal of Sound and Vibration, Volume 24, Number 1, 1972, pp. 63-85.

2. The American Rocket Company, "Space Transportation That Makes Sense for Tomorrow, Today. History, Capabilities, and Facilities," AMROC, June 1991.

3. Anderson, John D., Jr., Modern Compressible Flow, Second Edition, McGraw-Hill Publishing Company, New York, 1990.

4. Anderson, J. S., "The Effect of an Air Flow on a Single Side Branch Helmholtz Resonator in a Circular Duct," Journal of Sound and Vibration, Volume 52, Number 3, 1977, pp. 423-431.

5. Bruel & Kjœr, Condenser Microphones & Microphone Preamplifiers For Acoustic Measurements Data Handbook, Bruel & Kjaer, Naerum, Denmark, 1982.

6. Doebelin, Ernest O., System Modeling and Response, John Wiley & Sons, New York, 1980.

7. Dowling, A. P., & J. E. Ffowcs Ffowcs Williams, Sound and Sources of Sound, John Wiley & Sons, 1983.

8. Haberman, Richard, Elementary Applied Partial Differential Equations, Second Edition, Prentice-Hall, Inc., New Jersey, 1987.

9. Halliday, David & Robert Resnick, Fundamentals of Physics, John Wiley & Sons, 1988.

10. Hanly, Richard D., "Effects of Transducer Flushness on Fluctuating Surface OPressure Measurements", AIAA Paper Number 75-534, March, 1975.

11. Hoerner, Sighard F., Fluid-Dynamic Drag, Hoerner Fluid Dynamics, New Jersey, 1965.

12. Ingard, Uno, "On the Theory and Design of Acoustic Resonators," The Journal of the Acoustical Society of America, Volume 25, Number 6, November 1953, pp. 1037-1061.

13. Kinsler & Frey, Lawrence E. & Austin R. Frey, Fundamentals of Acoustics, Second Edition, McGraw-Hill Publishing Company, New York, 1962.

14. Lomen, David & James Mark, Differential Equations, Prentice Hall, New Jersey, 1988.

15. Miller, Richard W., Flow Measurement Engineering Handbook, Second Edition, McGraw-Hill Publishing Company, New York, 1989.

16. Morse, Philip M., & K. Uno Ingard, Theoretical Acoustics, McGraw-Hill Company, New York, 1968.

17. Panton, Ronald L., "Effect of Orifice Geometry on Helmholtz Resonator Excitation by Grazing Flow," AIAA Journal, Volume 28, Number 1, January 1990, pp. 60-65.

18. Panton, Ronald L. & John M. Miller, "Resonant Frequencies of Cylindrical Helmholtz Resonators," Journal Acoustics Society America, Volume 57, Number 6, Part II, June 1975, pp. 1533-1535.

19. Rayleigh, J. W. S., The Theory of Sound, Volumes I & II, Dover Publications, New York, 1945.

20. Sutton, George P., Rocket Propulsion Elements, Sixth Edition, John Wiley & Sons, Inc., New York, 1992.

21. Tang, P. K., & W. A. Sirignano, "Theory of a Generalized Helmholtz Resonator," Journal of Sound and Vibration, Volume 26, Number 2, 1973, pp. 247-262.

22. Van Santen, G. W., Mechanical Vibration, Elsevier Press Inc., Houston, TX, 1953.

23. Vennard, John K., Elementary Fluid Mechanics, Third Edition, John Wiley & Sons, Inc., New York, 1954.

APPENDICES

APPENDIX 1

ORIGINAL HYBRID ROCKET MOTOR DESIGN

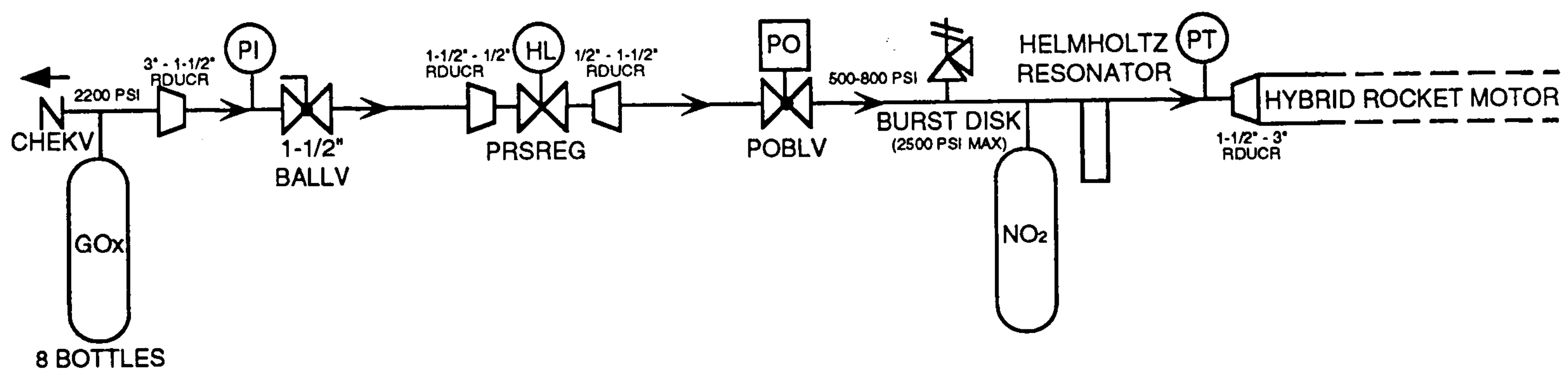

Figure A.1 Upstream Apparatus For Original Hybrid Rocket Motor Design

APPENDIX 2

CONDENSER MICROPHONE DATA

The intent of the Type 4136 microphone was for random incidence, coupler, high level and high frequency measurements. Figure A.1 presents the directional and distortion characteristics, and free-field correction curves for the Type 4136 Condenser Microphone (Bruel & Kjaer, 1982). The dynamic range of this microphone is:

DYNAMIC RANGE OF THE TYPE 4136

LOWER LIMIT OF THE SPECIFIED MAXIMUM NOISE

3, 16 Hz @ 1kHz:	19 dB
1/3-octave @ 1 kHz:	38 dB
A-weighted:	53 dB
Linear 20 Hz to 200 kHz:	64 dB

UPPER LIMIT OF THE SPECIFIED MAXIMUM NOISE

< 3% distortion:	172 dB
< 10% distortion:	180 dB

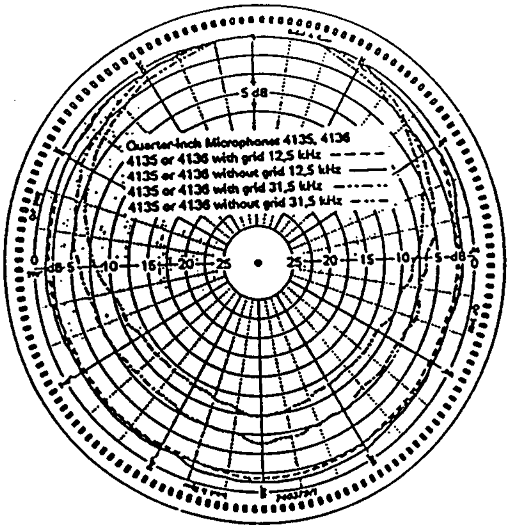

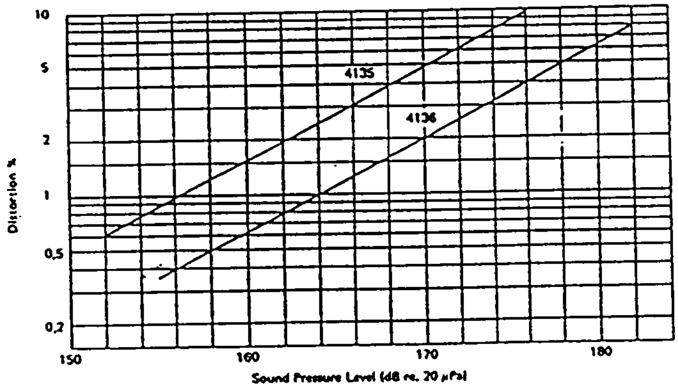

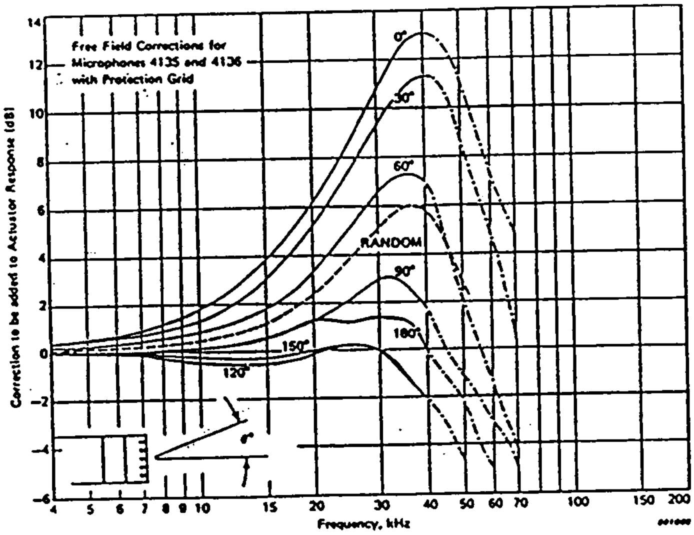

Free-field correction curves for quarter-inch Condenser Microphones Types 4135 and 4136 fitted with normal protection grid

Source: Bruel & Kjœr, Condenser Microphones & Microphone Preamplifiers For Acoustic Measurements Data Handbook, Bruel & Kjaer, Naerum, Denmark, 1982.

VITA

Patricia R. Taft was born in Meriden, Connecticut on May 23, 1960, and graduated from Mark T. Sheehan High School in Wallingford, Connecticut on June 22, 1978. From June 28, 1978, to February 17, 1986, she served in the United States Air Force, active duty, as a jet engine mechanic, departing as an E-5, Staff Sergeant. While in the service she served three years in Illinois, three years in Japan, and one year in upstate New York. She worked on various military engines including those on the C-5, C-141, T-39, C-140, FB-111, and C-130 aircraft.

Following the service Taft worked as a jet engine parts inspector of the PW2037 and JT8D engines at Pratt & Whitney Aircraft, in Southington, Connecticut, from April 14, 1986, to August 4, 1989. She also worked on A-10 jet engines while serving in the Connecticut Air National Guard from February 25, 1986, to October 15, 1986.

On August 8, 1988, Taft earned a bachelor of science degree in Vocational Education from Southern Illinois University. She left Pratt & Whitney on August 4, 1989, to attend Syracuse University full time, earning a bachelor of science degree in Aerospace Engineering, May 1992.

While attending Syracuse she earned several scholarships, including the $5000 Remembrance Scholarship, which honors one student for each Syracuse University student who died in the Pan Am Lockerbie airplane crash. She was inducted into both the Tau Beta Pi Engineering Honor Society and Sigma Gamma Tau Aerospace Engineering Honor Society

Taft attended The University of Tennessee Space Institute on a Space Grant Fellowship, August 1992 to May 1994, earning her Master's in Aerospace

Engineering.

Taft has been accepted, and plans to attend, Texas A&M University in the Fall 1994 semester in order to earn her doctorate in Atmospheric Science where she will study the effects El Nino has on the Earth's atmosphere.